

Age and petrogenesis of the Lundy granite: Palaeocene intraplate peraluminous magmatism in the Bristol Channel, UK

J.-H. CHARLES¹, M.J. WHITEHOUSE², J.C.Ø. ANDERSEN³, R.K. SHAIL³ & M.P. SEARLE¹

¹ Department of Earth Sciences, Oxford University, South Parks Road, Oxford, OX13AN, UK ² Swedish Museum of Natural History, Box 50007, SE-104 05 Stockholm, Sweden ³ Camborne School of Mines, College of Engineering, Mathematics and Physical Sciences, University of Exeter, Penryn Campus, Penryn, Cornwall, TR10 9FE, UK.

Abstract: The Lundy granite forms part of the Lundy Igneous Complex which is the southernmost substantive expression of the British Cenozoic Igneous Province (BCIP). Its Qz+Pl+Kfs+Bt±Grt±Tpz 16 mineralogy and peraluminous character contrast with other BCIP granites farther north but are similar to the granites of the adjacent Early Permian Cornubian Batholith. We present the results of mapping, petrographical and mineral chemical analysis, and the first U-Pb zircon ages for the granite ($59.8 \pm 19.0 - 58.4 \pm 0.4$ Ma) and cross-cutting basic dykes (57.2 ± 0.5 Ma) which confirm a Palaeocene age 20 for magmatism. Zircon inheritance is limited but two cores imply the presence of Lower Palaeozoic igneous rocks in the unexposed basement of SW England. The anomalous southerly location of the Lundy Igneous Complex is a consequence of mantle melting arising from the superposition of localised lithospheric extension, related to intraplate strike-slip tectonics, with the distal ancestral Icelandic plume. Granite generation primarily reflects crustal partial melting during the emplacement of mantle-derived melts. The change in geochemical character between the Lundy granite (peraluminous) and other BCIP granites (metaluminous / subalkaline) indicates a fundamental crustal source control between contrasting peri-Gondwanan and Laurentian basement provinces.

Introduction

Lundy Island (~4.5 km²) lies in the Bristol Channel, 20 km NNW of Hartland Point on the North 37 Devon coast (Fig. 1). It is composed predominantly (>90%) of two-mica ± garnet ± tourmaline 38 granite, hosted by Variscan-deformed Devonian low-grade metasedimentary rocks; both are cut by a 39 suite of basalt-dolerite, trachyte and rare rhyolite dykes (Dollar 1941; Edmonds et al. 1979;

Dangerfield 1982). Lundy is the only subaerial expression of the Lundy Igneous Complex that has a much larger subcrop in the Bristol Channel (Arthur 1989; Tappin et al. 1994).

Some early studies of the Lundy granite suggested it was an expression of the PermoCarboniferous Cornubian Batholith due to their proximity and mineralogical similarities (Davison 1932; Dollar 1941); others advocated a linkage with the granites of the British Tertiary Province due to the numerous cross-cutting dolerite dykes (McClintock & Hall 1912; Shelley 1966). A Palaeocene Rb-Sr whole rock isochron for the Lundy granite of 58.7 ± 1.6 Ma (Thorpe et al. 1990), combined with earlier whole-rock and mineral radiometric dating of granites and dolerites (Miller & Fitch 1962; Dodson & Long 1962; Edmonds et al. 1979; Mussett et al. 1976, 1988) indicated that the Lundy Igneous Complex is the most southerly substantive expression of the British Cenozoic Igneous Province (BCIP). In contrast, U-Pb monazite and xenotime ages, considered to date emplacement of the Cornubian Batholith, are Early Permian (298 – 273 Ma) (Chen et al. 1993; Chesley et al. 1993).

Whole-rock and mineral isotopic and geochemical studies have evaluated the roles of mantle- and crustal-melting, differentiation and contamination in generating the Lundy granite (Thorpe et al. 1990; Stone 1990) and basalt-trachyte-rhyolite dykes (Thorpe & Tindall 1992). Specifically, the Lundy granite has a relatively evolved Sr and Nd isotope signature, with $^{87}\text{Sr}/^{86}\text{Sr}$ ratios of ~ 0.715 , and ϵ_{Nd} values of -0.9 to -1.9 (Thorpe et al. 1990). Ytterbium, Nb and Rb trace element data indicate an affinity with ‘syn-collisional’ or ‘within-plate’ granites (Pearce et al. 1984).

The development of the Lundy Igneous Complex has been related to Palaeogene rifting in the North Atlantic Igneous Province and distal effects of the ancestral Iceland plume (White & McKenzie 1989; Kent & Fitton 2000). However, the occurrence of an igneous centre and granites 500 km S of the nearest BCIP granites in the Mourne mountains of Northern Ireland, is anomalous.

In this paper we first briefly describe the tectonic setting of Lundy with respect to the British Cenozoic Igneous Province. We then summarise the field relationships of the Lundy granite and associated dykes and discuss the whole rock geochemistry and newly obtained mineral chemistry. We present seven new U-Pb zircon ages for the granites and dykes that confirm a Palaeocene age for magmatism. Finally, we propose a model to explain the generation and emplacement of the Lundy granite and account for its similarities with the older granites of the Cornubian Batholith

British Cenozoic Igneous Province (BCIP)

Prior to the opening of the North Atlantic between $\sim 56 - 53$ Ma, regional outpouring of flood basalts occurred along the eastern margin of Baffin Island, along the west and east coasts of Greenland and the western margin of the British Isles. These flood basalts have been linked to both the Iceland hotspot and to magmatic underplating during rift-flank uplift (e.g. White & McKenzie 1989). In the British Isles, stretching of continental lithosphere initiated at c. 63 Ma and was subsequently accompanied by the eruption of dominantly basaltic lavas across a large area stretching from Rockall and St. Kilda, west of

the Outer Hebrides, east to Skye, Mull, Rum, Muck, Eigg and Arran, south to Ardamurchan and Ailsa Craig to the Mourne mountains, Slieve Gullion and Carlingford Lough in NE

Ireland (Fig. 1). Most of these basaltic volcanic rocks formed between ~61 – 59 Ma (Chambers & Fitton 2000). Primitive gabbros and layered peridotites are present in Rum and Skye that show compositional similarities to the Kap Edvard Holm and Skaergaard intrusions of SE Greenland (Wager & Brown 1968; Tegner et al. 2008). The layered gabbros and peridotites of Skye, Ardamurchan and Mull have been extensively intruded by basaltic cone sheets, and on Skye also by later granites (Red Hills granites).

Although 90% or more of the BCIP comprises transitional tholeiitic to mildly alkalic basaltic rocks, an important, yet volumetrically minor component is granitic. Strontium and lead isotopes show that the basalts are mantle-derived, while the granites were derived from partial melting of crustal sources (Moorbath & Bell 1965). The only U-Pb age from granites within the BCIP are the amphibole-bearing coarse-grained granites from the Mourne Mountains of NE Ireland that have U-Pb zircon ages of 55.3 ± 0.8 Ma and 56.4 ± 1.4 Ma (Gamble et al. 1999). Rb-Sr whole rock and mineral isochron ages for granites from St.Kilda (55 ± 0.5 Ma; Harding et al. 1984), Skye (59.3 Ma; Dickin 1981), Rum (59.8 ± 0.4 Ma; Mussett 1984), Arran 60.3 ± 0.8 Ma (Dickin 1981), Ailsa Craig (62.0 Ma; Harrison et al. 1987), Rockall ($57 - 54 \pm 4$ Ma; Hawkes et al. 1975) and Mull (58.2 ± 1.3 Ma; Chambers and Pringle, 2001) are shown on Fig. 1.

Kent and Fitton (2000) proposed that two mantle sources were present during the Paleocene, a mildly alkalic ‘Icelandic plume’ mantle and a N-type MORB outer envelope to the plume. They envisaged a massive ancestral Iceland plume head extending beneath Greenland to eastern Baffin Island in the west, and all the way beneath the British Isles to the east. The mantle-derived basalts were affected by fractional crystallisation and some degree of crustal contamination (Thompson & Morrison 1988). Heat from mantle derived melts was responsible for local crustal melting and the composition of the granites range from metaluminous (Skye, Mull) to peraluminous (Lundy) depending on the source rocks and melting regime (Thompson 1982)

Gravity and magnetic anomalies around Lundy

The British Geological Survey Bouguer gravity anomaly map of SW England clearly outlines the ESE-WNW alignment of the Cornubian batholith from the Scilly Isles to Dartmoor (Fig. 2). A separate parallel negative gravity anomaly approximately 46 km long and up to 14 km wide extends over the Haig Fras seamount; dredge samples and radiometric surveys confirm granites hosted by Devonian-Carboniferous slates and phyllites (Jones et al. 1988). The Haig Fras batholith represents a second parallel batholith north of the Cornubian batholith (Exley 1966).

The Lundy Igneous Complex is associated with a gravity anomaly of +23 mgal centred around a peak high 10 km WNW of the island coinciding with a circular positive magnetic anomaly. The total area of the anomaly is ~1500 km² and its magnitude is comparable to other igneous complexes in the BCIP

(Bott & Tuson 1973). The association of gravity and magnetic anomalies led Bott et al. (1958) and Brooks & Thompson (1973) to infer a mafic intrusion between 2.5 and 4 km thick lying at shallow depth to the WNW of Lundy. Gravity anomaly data are consistent with the Lundy granite approximating a circular laccolith with steep margins, a diameter of 4.8 km, a thickness of 1.6 km and a volume of ~30 km³ (Bott et al. 1958).

An additional magnetic low extending 30 km NW from a point 10 km NW of the island is reversely magnetised and interpreted as a Cenozoic dyke swarm (Cornwell 1971). The predominantly WNW-ENE striking doleritic dykes on Lundy Island are thought to be part of a local set of basic dykes aligned NW-SE in the Bristol Channel, parallel to the trend of similar Cenozoic basic dykes across western Scotland, northern England and Northern Ireland (Cornwell 1971; Roberts & Smith 1994). Two major NNW aligned steep extensional faults bound the Lundy Island horst, the Sticklepath-Lusteigh fault approximately 5 km east of Lundy, and the West Lundy fault approximately 12 km west of Lundy (Arthur 1989).

Field relations on Lundy

The Lundy granite is a relatively homogenous peraluminous granite. Although Dollar (1941) described two main types of medium to coarse grained megacrystic two-mica granites (G1 and G2), it is not possible to distinguish these as distinct mappable units in the field. The grey two-mica granites are variably megacrystic and locally display micrographic textures. They are cross-cut by subordinate pegmatites and microgranite sheets (Fig. 3). The microgranites and pegmatites appear as irregular patches, pods and dykes that in places appear to be internal segregations and in other places are distinctly intrusive (Fig. 4a). Small xenoliths of the Lundy Slate Series appear in the granite near the granite-slate boundary in the S of the island (Fig. 4b). The main Lundy granite is cut by a bimodal sequence of dolerite and trachyte-rhyolite dykes (Fig. 4c)

The low-grade metasedimentary rocks in the SE part of the island are composed of a succession of thick, folded and well-jointed arenaceous slates. Dollar (1941) correlated the Lundy Slate Series with the Upper Devonian Morte Slates of North Devonshire. The boundary between the granite and the metasedimentary rocks trends NNE-SSW and is at least partly fault controlled. At Ladies Beach (Fig. 4d) a fault zone crops out ~10 m from the boundary. The fault plane displays two clear sets of striations, indicating predominantly strike-slip movement. The contact on the western side of Rattles Anchorage (Fig. 4e) is heavily fractured, but its exact nature is uncertain due to inaccessibility. Edmonds et al. (1979) suggested that, in addition to the island's major strike-slip faulted contact, there may be an extensional contact, but this junction is cut by a basic dyke resulting in a high degree of brecciation. The trace of the fault boundary appears approximately linear, despite no exposure inland, suggesting that the fault is nearly vertical as observed at Ladies Beach. A faulted contact between the granite and Lundy Slate is consistent with the lack of thermal metamorphism in the metasedimentary rocks and absence of granite veining.

Over 200 dykes (average thickness 1 m, up to 4 m) (Dollar 1941) with varying compositions from intermediate to basic (90% of the dyke swarm is basic) cross-cut the granite and Lundy Slate Series. The dykes post-date the solidification of the granite and have been emplaced into joints across the island. There is limited disruption at dyke-host rock boundaries and where brecciation occurs, it affects a limited area (<2 cm from contact). Field relations suggest all dyke compositions were emplaced contemporaneously during regional NNE-SSW extension. Extrapolation of the distribution pattern suggests a possible focus and melt source 2 – 3 km W of the island. (Roberts & Smith, 1994) This is roughly coincident with the positive gravity anomaly located to the NW of the island identified by Brooks & Thompson (1973). The characteristics of the Lundy dyke swarm are commonly compared with the dyke swarms of central intrusive complexes within the BCIP, for example Ardnamurchan (Speight et al. 1982). Edmonds et al. (1979) suggest that the dykes may be a southeasterly extension of the NW-SE dyke swarm described in the regional magnetic survey by Cornwell (1971).

Sampling and petrography

Thirty-two samples were collected from the range of exposed lithologies on Lundy. Thin sections were studied from all samples and their petrography is detailed below.

Coarse-grained megacrystic biotite granite

The main Lundy granite (~70% of exposures) is a hard white-grey coarse-grained megacrystic granite composed of around 39% quartz, 33% K-feldspar, 26% plagioclase, 2% micas and sporadic garnet and tourmaline (cf., Edmonds 1979). K-feldspar megacrysts locally reach up to ~20% and contain complex zones with quartz inclusions, as described by Shelley (1966), in addition to myrmekitic quartz growths at some feldspar boundaries. Locally quartz forms rounded, subhedral megacrysts (3 – 10 mm). Interstitial anhedral quartz crystals (0.1 – 0.3 mm) display undulose extinction. Plagioclase is generally lamellar twinned, and commonly displays patchy replacement by K-feldspar and alteration to sericite. Biotite occurs in clusters as well as isolated sub-euhedral laths, and is partially altered to chlorite and muscovite. Locally garnets occur (up to 6 mm diameter), rimmed by quartz and micas against the groundmass. Fractures in the garnet are locally infilled by green biotite (Stone, 1988). Accessory and secondary minerals are particularly abundant in the region near the contact with the Slate Series, including garnets, tourmaline, beryl, cassiterite and topaz. Some small psammitic xenoliths are also present. Strain features in the granite are observed at the junction with the Slate Series [SS 1350 4350]; planar microfractures in all minerals, undulose extinction in quartz grains, deformation twinning and curvature in feldspars, and flexure and planar failure in muscovite (Dollar, 1941). Four samples from this lithology have been dated in this study (LY4, LY21, LY25 and LY29).

Medium to fine-grained megacrystic biotite granite

The medium to fine-grained megacrystic biotite occurs as pods and patches within the coarse-grained megacrystic biotite granite. Its mineralogy and composition is similar but megacrysts (average content ~40%), comprise zoned plagioclase (5 – 20 mm) and sub-euhedral K-feldspar (mean 19 – 24 mm, up to 50 mm). It also displays zones of blebby, sub-euhedral quartz which are commonly composed of several sutured grains. Edmonds et al. (1979) suggested that the main distinction between the two main megacrystic granite styles is ‘the presence or absence of bipyramidal quartz’. The groundmass contains plagioclase, K-feldspars, quartz, biotite and colourless mica and has an average grain size of 0.1mm (range 0.03 – 3 mm). One sample from this lithology has been dated in this study (LY22).

Microgranite (fine-grained poorly megacrystic granite)

Two microgranites are present: a leucocratic facies, and a more melanocratic, biotite-rich facies. Generally composed of finely intergrown feldspar and quartz, with biotite subordinate to muscovite. Rhythmic banding according to mineralogy and grain-size is common, especially in association with pegmatites.

Lundy dykes

The dykes are dominantly olivine basalts – dolerites (90% of exposures) with subordinate peralkaline trachytes and rhyolites containing K-feldspar + quartz + amphibole ± clinopyroxene. The dykes display considerable variation in grain size and texture (porphyritic and aphyric).

Most dolerites are porphyritic, containing scattered phenocrysts. Commonly zoned, subeuhedral plagioclase feldspar phenocrysts (1 – 10 mm) are dominant and may contain inclusions. Olivine phenocrysts are observed with euhedral-subhedral forms (0.08 mm and 0.5 mm), with partialcomplete alteration to serpentine group minerals and chlorite. Some dolerite dykes display vesicularity suggesting a shallow emplacement depth. The dolerite dykes contain no zircon and were thus not amenable to dating in this study.

Felsic dykes are dominated by quartz trachytes. They are commonly medium-fine grained to fine-grained, pale-greenish-grey colouration and pale-brown to buff weathering with intergranular, orthophyric textures. Most specimens contain some phenocrysts (average content: 7%), although they are not generally porphyritic. Phenocrysts are generally K-feldspars with elongate laths (1.5 – 6 mm). Groundmass is commonly microcrystalline. Plagioclase has generally undergone K metasomatism and perthitisation to develop K-feldspars and interstitial quartz (elongate laths 0.1 – 0.25 mm). Two dyke samples were dated in this study (trachyte LY13 and felsite LY32).

Whole rock geochemistry

The main Lundy granite is peraluminous ($\text{Na}_2\text{O} \sim 3 - 4\%$, $\text{K}_2\text{O} \sim 5\%$, Al_2O_3 12 –14%) (Thorpe et al. 1990) with major element characteristics similar to the S-type granites of White & Chappell (1988). We concur with Edmonds et al. (1979) and Thorpe et al. (1990) who showed that there is no geochemical distinction between the G1 and G2 granite types of Dollar (1941). The Lundy granite exhibits higher SiO_2 (71 – 76%) and lower TiO_2 (<0.1%), MgO and CaO than average continental granites, and the Cornubian and BCIP granites. It has high Rb and Li and is halogen-rich like the syn- to post-collisional Cornubian granites (Exley & Stone 1982; Exley & Floyd 1983; Darbyshire & Shepherd 1985; Charoy 1986). The main Lundy granite has lower Sr, Ba, Zr, K/Rb, REE and Ce/Y; higher Rb, Nb, Sn, Ta, Eu/Eu* (Edmonds et al. 1979; Stone 1990). In tectonic discrimination diagrams (Pearce et al., 1984), Lundy granites plot separately from the Cornubian granites and in the within plate-plate field in Nb vs. Y (Fig. 5).

The REE patterns are flat relative to other granite suites. The Lundy granite displays a large negative Eu anomaly, similar to that of the Mourne Mountain granites (Meighan et al. 1984); the microgranites and pegmatites are further REE depleted, but display a similar REE pattern. The Lundy granite has high $^{87}\text{Sr}/^{86}\text{Sr}$ ratios (0.734) (Dodson & Long 1962)

Thorpe & Tindle (1992) reported that the major element chemistry of the dykes is characteristic of anorogenic bimodal dolerite/ basalt and minor trachyte/ rhyolite associations. Stone (1990), investigated the whole-rock geochemistry of the basic rocks and noted that, in comparison to the 'average' basic compositions proposed by Manson (1967) and Prinz (1967), they display average Al_2O_3 , high Fe_2O_3 , highly variable FeO, low MgO , CaO , K_2O and trace elements, which have scattered but generally low Cr, Ba, Ni, Rb, Sr (Edmonds et al. 1979).

Mineral Chemistry

Samples of all the major lithologies on Lundy were collected and thin-sectioned for further petrographic analysis. With the exception of garnet and tourmaline, the analysed minerals are ubiquitous to all granite facies on Lundy. Carbon-coated thin-sections were analysed using a JEOL JXA-8200 Superprobe at the University of Exeter, Camborne School of Mines using an electron beam intensity of 30 nA and an acceleration voltage of 15 kV. Analyses were referenced to natural silicate and oxide mineral standards. Signal intensities were collected over 20 s with 10 s on the each of two background positions (increased to 40 s peak and 20 s background for minor elements). The matrix correction procedure follows the phi-rho-Z routine by Armstrong (1995) and implemented by Paul Carpenter.

Garnet

Garnet occurs only in the coarse-grained megacrystic biotite granite and was analysed from samples LY15, LY21 and LY25. Almandine dominates, with the approximate composition

$\text{Alm}_{81}\text{Sp}_{10}\text{Pyr}_4\text{Gro}_5$, as expected for peraluminous biotite granites (Stone 1988). Major element zoning (Fig. 6) has Mn and Mg steadily decreasing towards the rim and Fe increasing, consistent with magmatic fractionation under falling temperatures or retrograde re-equilibration with the evolving magma (Artherton 1968; Hollister 1966). Some garnets are fractured, at temperatures high enough for replacement along fractures by biotite. The garnets are compositionally similar to those from the Dartmoor granite, except for their lower Ti, Mg and Cl; higher Mn, F; marginally higher Rb, Cs and Fe and much higher $(\text{Fe}+\text{Mn})/(\text{Fe}+\text{Mn}+\text{Mg})$ (Stone 1988).

Biotite

Biotite was analysed in samples LY2, LY3, LY4, LY15, LY17, LY18 and LY20. Protolithionites and siderophyllites define a linear cluster in the $\text{Fe}+\text{Mn}+\text{Ti}-\text{Al}^{\text{IV}}$ vs Mg-Li diagram of Tischendorf et al. (2001). Biotite in the coarse-grained megacrystic biotite granite plots across this cluster with no systematic compositional association. Protolithionite predominates in the medium-grained poorly megacrystic granite, whilst siderophyllite predominates in the microgranite. Protolithionites are exposed rarely in the UK (only at St. Austell, Tregonning-Godolphin and Glen Gairn), and hold an affinity with Sn-W mineralisation. Biotite crystals occur in cracks in garnet, coexisting in a host present as replacement minerals. These biotites are siderophyllites and are richer in Mg, and poorer in Ti than matrix biotite. Mica contents within individual samples exhibit significant variability and clustering, with a possible bimodal distribution of two distinct populations (Fig. 7).

Muscovite

Muscovite was analysed in samples LY2, LY3, LY4, LY15, LY17, LY18 and LY20. These analyses occupy two compositional clusters in the Tischendorf et al. (2001) $\text{Fe}+\text{Mn}+\text{Ti}-\text{Al}^{\text{IV}}$ vs Mg-Li diagram; secondary late-post magmatic ferroan polyolithionite which has partially overgrown lithian siderophyllite, and primary muscovite. There is no systematic relationship between granite facies and muscovite composition. Muscovites are clearly phengitic, and ‘contain 10 – 20% celadonite component’ (Stone 1990). Lundy muscovites exhibit high tFeO, high MnO, Rb_2O and high F (Stone 1990).

Alkali feldspar

Alkali feldspar was analysed in samples LY2, LY3, LY4, LY15, LY17, LY18, LY20, LY21, LY22, LY23, LY25, LY29 and LY30. The average alkali feldspar megacryst composition is $\text{Or}_{83}\text{Ab}_{17}$, within a compositional range of Or_{70} to Or_{90} . The megacrysts are microperthitic and therefore approximately 10% of analytical data were albitic. There is no distinct intra-sample variation between megacryst composition, nor between samples in different locations (Stone 1990; Thorpe et al. 1990). The mineral textures within K-feldspar phenocrysts are notable, with zonal arrangements of plagioclase and quartz inclusions (Shelley 1966). Thorpe et al. (1990) determined alkali feldspar megacrysts to have low Sr, Ba and high Rb/Sr and Eu/Eu*.

Plagioclase

Plagioclase was analysed in samples LY2, LY3, LY4, LY15, LY17, LY18, LY20, LY21, LY22, LY23, LY25, LY29 and LY30. The average composition of plagioclase megacrysts is $Ab_{92}An_8$, within a compositional range of $Ab_{81}An_{19}$ to $Ab_{99.5}An_{0.5}$. The compositional range is associated with normal zoning variation (Stone 1990).

Tourmaline

Tourmaline occurs only as a minor accessory mineral in localised areas (e.g. at SS 1340 4350) of the finely-grained megacrystic granite and was analysed from sample LY30. It is euhedral, with crystal dimensions up to 20 mm. The tourmaline analysed belongs to the alkali group, and is classified as a schorl according to the scheme of Hawthorne & Henry (1999). The tourmaline displays two distinct zones (Fig. 8) with $Mg/(Mg+Fe)$ ratios at 0.01 (core, C and B) and 0.1 (A), closely similar to some of the most evolved granites in the Cornubian Batholith (cf., Müller et al., 2006). However, the Ti and Ca contents are substantially different from the main Cornubian granite trend and display closer similarity with the massive quartz-tourmaline rocks (Müller et al., 2006; Drivenes et al., 2015). Lithium concentrations (estimated using the technique of Burns et al., 1994) are relatively low, with $Li_2O < 0.2$ wt%.

The compositional trend of tourmaline appears to be mainly related to the coupled exchanges of $(Fe)(Mg)_{-1}$ comparable to some of the most evolved tourmaline in the Cornubian batholith. Minor differences in Ca and Ti could reflect differences in the melting regime during granite formation, or a localised hydrothermal signature (Müller et al., 2006; Drivenes et al., 2015).

U-Pb zircon geochronology

Analytical Method

Five samples of granite and two dykes, chosen to be geographically and texturally representative of the island, were selected for U-Pb Secondary Ion Mass Spectrometer (SIMS) zircon dating. Cleaned samples were mechanically disaggregated in an agate swing mill and screened to < 300 μm , prior to heavy mineral extraction via water table, magnetic and heavy liquid (methylene iodide) separation. Zircon grains were hand-picked from the heavy mineral fraction onto double-sided tape and cast together with pieces of the Geostandards 91500 zircon (Wiedenbeck et al., 1995) into epoxy resin. Following polishing and cleaning, the internal structures of the grains were documented by cathodoluminescence (CL) on a FEI XL30 ESEM equipped with a Centaurus CL detector at the Swedish Museum of Natural History and then coated with 30 nm of gold for SIMS analysis.

U-Th-Pb analyses were performed on a CAMECA IMS1280 large-geometry ion microprobe at the Swedish Museum of Natural History (NordSIMS facility). Analytical protocols closely follow those

described by Whitehouse et al. (1999) and Whitehouse & Kamber (2005). $^{238}\text{U}/^{206}\text{Pb}$ ratios were calibrated from raw ratios using in-house developed routines that apply an empirical power-law relationship between $^{206}\text{Pb}^+ / ^{238}\text{U}^{16}\text{O}^+$ and $^{238}\text{U}^{16}\text{O}_2^+ / ^{238}\text{U}^{16}\text{O}^+$. The overall analytical uncertainty propagates observed errors on measured Pb/U ratios with the external error from replicate analyses of the standard (typically < 1%, SD). Corrections for non- in situ radiogenic (common) Pb were made when $^{204}\text{Pb}^+$ counts exceeded three times the standard deviations in the ion counting detector background, assuming the present-day terrestrial Pb isotope model composition of Stacey and Kramers (1975); analyses with a common ^{206}Pb content in excess of 3% were omitted from further consideration. Age calculations use the decay constant recommendations of Steiger and Jäger (1977) and utilise routines of Isoplot-Ex (Ludwig, 2012). U-Th-Pb analytical data for zircon samples are presented in Tera-Wasserburg concordia plots ($^{207}\text{Pb}/^{206}\text{Pb}$ vs. $^{238}\text{U}/^{206}\text{Pb}$) (Fig. 10). All ages are presented at 2σ or 95% confidence, with the MSWD (mean squared weighted deviation) representing that of both concordance and equivalence, following the recommendation of Ludwig (1998).

Lundy granites

The morphology of zircon grains separated from the Lundy granite is generally consistent across the five studied samples. Grains are typically up to 200 μm in length, euhedral, equant to prismatic, with well-developed facets and some are clearly fragments of larger grains broken during processing. In cathodoluminescence (Fig. 9) they vary from medium to bright luminescence and mostly display well-defined oscillatory, typically igneous, zoning. In some cases this zoning mantles an unzoned central region, reflecting a likely evolution in zircon crystallisation conditions. Clearly polyphase grains with distinct cores are rare, and in many cases CL-distinctive inner regions of the grain are of the same age as their outer regions. In a few cases, disruption of the oscillatory zoning probably reflects late-stage magmatic processes.

LY4: Coarse-grained megacrystic biotite granite

Twenty-three analyses were performed on unique grains. The grains display a wide range in U content of 100 to 2300 ppm, although only two exceed 630 ppm. Th/U ratios also exhibit a wide range (0.06 – 1.3) and while the two highest U analyses have the lowest Th/U, this range is exhibited by the entire population. Omitting two analyses with very high common Pb, which may have sampled inclusions, and a slightly discordant analysis, nineteen analyses yield a concordia age of 58.8 ± 0.4 Ma (95% confidence, MSWD = 1.2), interpreted as the crystallisation age of the granite. A single inherited core identified in CL yielded a 50% discordant analysis with a minimum $^{207}\text{Pb}/^{206}\text{Pb}$ age of 482 ± 48 Ma (assuming modern loss).

LY21: Coarse-grained megacrystic biotite granite

Thirty analyses were performed on twenty-nine grains. Uranium concentration in the main population ranges from 57 to 1250 ppm, with Th/U ranging from 0.07 to 1.3; as noted for sample LY4, the Th/U range is largely independent of U concentration. Omitting one analysis with very high common Pb, twenty-eight analyses, including the rim of the older core, yield a concordia age of 58.7 ± 0.3 Ma (95% conf., MSWD = 1.3); further omission of one slightly older (inherited?) grain from this population results in a concordia age of 58.5 ± 0.3 Ma (2σ , MSWD = 1.0), interpreted as the crystallisation age of the granite. A single core identified in CL yielded a concordant $^{206}\text{Pb}/^{238}\text{U}$ age of 443 ± 28 Ma

LY22: Medium to fine-grained megacrystic biotite granite

Twenty-one analyses were performed on eighteen grains. Three “core/rim” pairs were targeted on the basis of marked CL contrast but no inherited older zircon was detected. Uranium concentration ranges from 140 to 2400 ppm (1340 ppm omitting the highest), with Th/U ranging from 0.06 to 2.3 (1.4 omitting the highest), the lowest ratio being associated with the highest U ppm and vice-versa. Rejection of two discordant analyses permits calculation of a concordia age of 58.9 ± 0.7 Ma (2σ , MSWD = 0.9), interpreted as the crystallisation age of the granite.

LY25: Coarse-grained megacrystic biotite granite

Twenty-nine analyses were performed on unique grains. Uranium concentration ranges from 60 to 770 ppm, with Th/U ranging from 0.14 to 3.1; as in LY22, the lowest ratios are typically associated with the highest U concentrations and vice-versa. All analyses are combined to yield a concordia age of 58.4 ± 0.4 Ma (95% confidence, MSWD = 1.4), interpreted as the crystallisation age of the granite.

LY29: Coarse-grained megacrystic biotite granite

Nineteen analyses were performed on eighteen grains. A single “core/rim” pair was targeted on the basis of marked CL contrast but revealed no inheritance. Uranium concentrations range from 61 to 8050 ppm, although only two exceed 980 ppm, while Th/U ratios range from 0.03 to 1.4, the lowest values associated with the highest U contents. Two analyses were discarded from further consideration due to their high common Pb content. A further three grains were omitted from the concordia age calculation, two on the basis of very high U contents (>3000 ppm) that result in artificially older ages (a well-documented SIMS phenomenon, e.g. McLaren et al. 1994) and one that is clearly younger and may have experienced minor Pb-loss. The remaining fourteen analyses define a concordia age of 59.8 ± 0.4 Ma (2σ , MSWD = 1.1), interpreted as the crystallisation age of the granite.

Lundy basic dykes

Zircon grains extracted from the basic dykes are generally smaller than those of the granite, rarely exceeding 100 μm in length, and commonly have equant to stubby prismatic forms.

Cathodoluminescence imaging (Fig. 9) shows a very uniform population of structureless to weakly zoned grains in sample LY13, with low to medium brightness and no evidence for older cores. The few grains recovered from LY32 exhibit a diversity in CL from grains closely resembling those in LY13 to strongly oscillatory zoned, CL-bright grains and it seems likely that some of these grains are xenocrysts.

LY13: Trachyte

Thirty-nine analyses were performed on thirty-eight grains, the single “core-rim” pair targeted on the basis of CL contrast revealing no inheritance. Uranium concentrations shows a more restricted range from 310 to 1430 ppm, with corresponding Th/U ratios from 0.49 to 1.7 and, in contrast to the granites, there is no correlation between these two parameters. Following rejection of five analyses with high common Pb, the remaining thirty-four analyses yield a concordia age of 57.2 ± 0.5 Ma (2σ , MSWD = 1.0), interpreted as the crystallisation age of the dyke.

LY32: Felsite

Nine analyses were performed on unique grains. In contrast to zircon from dyke sample LY13, U concentrations in zircon from LY32 exhibit a wide range from 112 to 4800 ppm, with Th/U ranging from 0.19 to 1.3; as with dyke sample LY13, there is again with no correlation between these parameters. Following rejection of two analyses with high common Pb and an additional analysis with high U concentration (3100 ppm), which is likely to be too old (e.g. McLaren et al. 1994), six analyses yield a concordia age of 57.3 ± 0.8 Ma (2σ , MSWD = 1.0). The likelihood of xenocrystic zircon suggested by the diverse CL characteristics of zircon from LY32 means that interpretation of this age as representing actual crystallisation is equivocal, but it does provide a maximum age for this event.

Discussion

Age and origin of the Lundy Igneous Complex

The U-Pb zircon ages from five samples of the Lundy granite range from 59.8 ± 0.4 Ma to 58.4 ± 0.4 Ma (Fig. 11). The ages of the oldest and three youngest granite samples do not overlap at a 2σ uncertainty, suggesting that the granite was emplaced in at least two episodes over approximately 2 Ma. The basic dykes intruding the granite are demonstrably younger at $c. 57.2 \pm 0.5$ Ma (Fig. 11). These new high-precision U-Pb zircon ages confirm a Palaeocene age for the development of the Lundy Igneous Complex and hence magmatism in the southernmost sector of the BCIP.

The Lundy Igneous Complex has been interpreted as an expression of Palaeogene rift and plume-related magmatic activity along the western margin of the British Isles prior to the onset of North Atlantic seafloor spreading (e.g. White & McKenzie 1989; Kent & Fitton 2000). However, the reasons for the development of a Palaeocene igneous centre in this anomalous southerly location are poorly understood. An association with the distal ancestral Icelandic plume was proposed on the basis that

Lundy basalt/dolerite dyke ΔNb values exhibited similarities with plume-influenced M1/M2 magma types further north (Kent and Fitton 2000). Such a suggestion is consistent with zones of anomalously low upper mantle seismic velocities beneath the North Devon / Bristol Channel area interpreted to be a consequence of asthenosphere-lithosphere re-equilibration following plume activity (Arrowsmith et al. 2005).

Major NW-SE crustal-scale strike-slip fault zones near Lundy, the Sticklepath-Lustleigh Fault Zone and West Lundy Fault Zone (Arthur 1989) may have passively controlled the transport of mantle plume-derived melts into and through the crust in much the same way as N-S faults influenced the location of some BCIP igneous centres in Scotland (Emeleus & Bell 2005). The 30 km long NWSE magnetic low that ends 10 km NW of Lundy, interpreted as a Cenozoic dyke swarm (Cornwell 1971), may reflect the influence of the Sticklepath-Lustleigh Fault Zone on magma transport and emplacement (Brooks and Thompson 1973).

However, the location of the Lundy Igneous Complex has also been attributed to the development of a rhomb graben during substantial early Cenozoic sinistral displacement across these NW-SE fault zones (Arthur 1989). Such localised lithospheric extension could have initiated mantle decompression melting that would occur more readily at the higher asthenosphere temperatures associated with a mantle plume. Such a model can account for the local generation and emplacement of *c.* 2000 km³ of basaltic melt, as indicated by the gravity and magnetic anomalies, into the attenuated crust around the Lundy rhomb graben, (Bott et al. 1958; Brooks and Thompson 1973; Arthur 1989). We contend that the anomalous southerly location of the Lundy Igneous Complex within the BCIP is likely to be a consequence of the superposition of localised lithospheric extension, related to intraplate strike-slip tectonics across the Sticklepath-Lustleigh and West Lundy fault zones, with the distal ancestral Icelandic plume.

The generation of the Lundy granite and dykes

The emplacement of mantle-derived basaltic melts within the continental crust about the Lundy rhomb graben initiated crustal partial melting and the generation of acid magmas (e.g. Huppert & Sparks 1988; Annen et al. 2006). Models for the generation of the Lundy granite (Thorpe et al. 1990) and granites elsewhere in the BCIP (Thompson 1982) involve variable mixing of variably fractionated granitic and basaltic magmas. A continental crustal source is consistent with the whole-rock and mineral chemistry, the abundance of garnet and biotite (Dodson & Long 1962; Hampton & Taylor, 1983) and rare inherited Lower Palaeozoic zircons. Sr and Nd data exclude the possibility that the Lundy granite resulted solely from the extreme differentiation of a basalt magma (Stone 1990). Although ¹⁴³Nd/¹⁴⁴Nd ratios indicate some equilibration with mantle derived material, the low TiO₂, MgO and CaO preclude a substantial contribution (Thorpe et al. 1990).

The emplacement of the Lundy granites was accompanied by host rock interactions that account for sedimentary xenoliths close to the granite margins and, possibly, minor ductile shear zones within

the southern granite. Following the emplacement and cooling of the main granite body, late microgranites with biotite and accessory minerals were generated by fractional crystallisation (Stone 1987; Stone & Exley 1989). The microgranites are REE depleted relative to the main granite, but display a similar REE pattern, indicating a common origin and lack of disturbance by hydrothermal processes.

The final stage of magmatism on Lundy involved the emplacement of doleritic, trachytic and felsitic dykes. Sr and Nd isotope data indicate the dyke magmas were derived from a BCIP-style mantle source (Thorpe & Tindle, 1992) and preclude the involvement of crustal material. The major and trace element characteristics of the dyke suite suggest that they are cogenetic and produced by low pressure (<2.5 kbar) fractional crystallization of a basic magma (Thorpe & Tindle 1992). The major basic body is thought to have remained active over a limited temporal window (*c.* 2.5 Ma) in a locally complex, small-scale magmatic plumbing system.

Zircon inheritance in the Lundy granite

The Lundy granite shows signs of petrological disequilibrium; micas display substantial compositional variability and garnets display zoning and possibly reaction rims (Fig. 6 & 7). These characteristics are consistent with partial equilibration of restite. However, zircon inheritance is rare and revealed by single Early Palaeozoic cores in each of two samples: Cambrian to Silurian in sample LY4 (strongly discordant, hence a minimum age) and Ordovician to earliest Devonian in sample LY21. These ages confirm that Lower Palaeozoic igneous rocks are present within the unexposed basement of SW England, and are in permissive agreement with a peri-Gondwanan origin and subsequent location on the margins of the Rheic Ocean (e.g. Woodcock et al. 2007; Shail & Leveridge 2009), but they do not constrain an Avalonian or Megumian affinity (Nance et al. 2015).

Comparison of Lundy granite to other BCIP granites

The Lundy Igneous Complex shares similarities with other BCIP igneous complexes. Geophysical characteristics (positive gravity and magnetic anomalies) interpreted as shallow basic intrusions (Bott et al. 1958; Brooks & Thompson 1973), association with a regional dyke swarm (Cornwell 1971) and limited granite thickness (Stone 1990). The Lundy granite differs from other BCIP granites in its strongly peraluminous character, locally abundant garnet, and the presence of Li-micas and tourmaline. The granites of Arran and the Mourne Mountains are metaluminous and subalkaline (Stone, 1990). The clinopyroxene, amphibole and titanite that occur in other BCIP granites are absent from the Lundy granite (Stone 1990). The whole rock geochemistry has lower Zr, Ba, Sr and higher Rb, Rb/Sr and Eu/Eu* (Thorpe et al. 1990) which is consistent with a source that is poorer in the HFSE and richer in K-feldspar and micas.

Comparison of Lundy granite to the Cornubian batholith

The Early Permian Cornubian batholith comprises peraluminous granites primarily derived from partial melting of metasedimentary rocks (e.g. Charoy 1986; Chen et al. 1993; Chappell & Hine 2006; Simons et al. 2016). The granites were generated during post-Variscan extension when substantial partial melting of the lower crust was driven by the emplacement of mantle-derived melts (Simons et al. 2016); lamprophyre and basalt dykes and lavas are broadly coeval with batholith construction (Dupuis et al., 2015). Two-mica, muscovite, biotite, and tourmaline-bearing granites resulted from muscovite-dominated (731 – 806°C, >5 kbar) and biotite-dominated (768 – 847°C, <4 kbar) dehydration melting reactions (Simons et al. 2016). Younger topaz granites are chemically distinct and related probably to later F, Li, P and HFSE rich fluids (Simons et al. 2016). The granites are associated with extensive magmatic-hydrothermal Sn and W mineralisation (Romer & Kroner 2016).

The strong mineralogical and chemical similarities between the Lundy granite and Cornubian batholith were recognized by Davison (1932) and Dollar (1941) and were most recently addressed by Stone (1990) and Thorpe et al. (1990). These similarities include S-type granite characteristics (Chappell & White 1974), mineral assemblage e.g. muscovite, biotite, (tourmaline, garnet, topaz), geochemical affinities (peraluminous, high Al saturation index, high Rb, Rb/Sr and Li, high trace alkali, Nb, U and F, low Zr, K/Rb and high initial Sr ratio), implying a high crustal anatectic component, textural features (coarse-grained megacrystic biotite granite with microgranites), biotite chemistry and tin mineralisation (Stone, 1990). Zircon inheritance in the Cornubian batholith also appears limited but the available data indicate late Devonian and Mesoproterozoic components (Neace et al. 2016). There are key differences between the Cornubian Batholith and Lundy granite in scale, geophysical characteristics (no similarity between gravity and magnetic anomalies), whole rock and trace element geochemistry, and mineral chemistry (Stone 1990). The Lundy granite also appears to have no metamorphic aureole, in contrast to the Cornubian Land's End granite for example (Pownall et al. 2012), and there are no contemporaneous lamprophyric dykes on Lundy.

Contrasting crustal sources during generation of BCIP granites

Crustal melting, primarily induced by emplacement of mantle-derived magmas has generated the peraluminous granites of Lundy and the Cornubian batholith at different times and in different tectonic regimes (intraplate vs post-orogenic). The BCIP granites of Ireland and Scotland, formed at the same time and in the same intraplate setting as the Lundy granite, but are dominantly metaluminous. We consider that these contrasts in character of the BCIP granites relate to a dominant crustal source control on the geochemistry of the magmas (e.g. Clemens and Stevens 2012). The peraluminous character of the Lundy and Cornubian granites is a consequence of partial melting of a crustal source that included metagreywackes and/or metapelites (e.g. Thorpe et al. 1990; Simons et al. 2016). Limited zircon inheritance in both cases is consistent with high crustal melting temperatures associated with the emplacement of mantle-derived melts. It is not possible to conclude that the Lundy crustal source was

identical to that for the Cornubian Batholith. Contrasts in lead isotope characteristics were highlighted by Thorpe et al. (1990) and, though sampling is inadequate, rare Mesoproterozoic inherited zircons in the Cornubian Batholith (Neace et al. 2016) contrast with Lower Palaeozoic inherited zircons in the Lundy granite. However, the unusual enrichment in Li and B and association with Sn mineralisation is one of the characteristics of peri-Gondwanan terranes such as Avalonia and SW England (Romer & Kroner 2014). In contrast, all other BCIP granites, located north of the Iapetus suture, were sourced from Laurentian crust which has no such enrichments.

Conclusions

- 1) We have presented the first U-Pb zircon age determinations for the exposed part of the Lundy Igneous Complex; these confirm a Palaeocene age for magmatism in this southernmost sector of the BCIP. The Lundy granite U-Pb zircon ages range from 59.8 ± 0.4 Ma to 58.4 ± 0.4 Ma range whilst the cross-cutting dykes are *c.* 57.2 ± 0.5 Ma.
- 2) Zircon inheritance in the Lundy granite is rare and revealed by single Early Palaeozoic cores in only two samples; these imply the presence of Lower Palaeozoic igneous rocks within the unexposed basement of SW England.
- 3) Generation of the Lundy granite was primarily driven by emplacement of mantle-derived basaltic melts into crust. The peraluminous character of the Lundy granite contrasts with other BCIP granites that are metaluminous or subalkaline but is similar to the Early Permian Cornubian Batholith. We consider that this reflects a fundamental crustal source control on granite composition between the Laurentian terranes north of the Iapetus suture (BCIP granites of Scotland and Ireland) and peri-Gondwanan terranes on the margins of the Rheic suture (cf. Clemens & Stevens 2012; Romer & Kroner 2014; Simons et al. 2016).
- 4) The anomalous southerly location of the Lundy Igneous Complex within the BCIP is likely to be a consequence of the superposition of localised lithospheric extension, related to Palaeocene intraplate strike-slip movement across the Sticklepath-Lusteleigh and West Lundy fault zones (Arthur, 1989), with the distal ancestral Icelandic plume (Kent and Fitton 2000).

Acknowledgements

Journal reviews by Fernando Corfu and an anonymous reviewer are gratefully acknowledged. Thanks to The Landmark Trust and Natural England for permission to undertake fieldwork on Lundy.

Financial assistance was received from University College Oxford, the Geologists' Association, the Lundy Field Society and the Burdett-Coutts fund. Thanks also to Steve Pendray, Beth Simons, Gavyn Rollinson and Joe Pickles at the Camborne School of Mines for their advice and help with analysing and conducting electron probe microanalysis, to Andy Tindle for the use of his mineral recalculation software and to Kerstin Lindén, Lev Ilyinsky and Per-Olof Persson for their advice and help with

zircons and geochronology at the NordSIMS laboratory in Stockholm. This is NordSIMS contribution ###.

Figure Captions

Fig. 1. Map of the British Isles showing locations of the main Cenozoic igneous intrusions, with age data. Granite complex ages compiled from: St Kilda - Brook 1984; Skye - Dickin, 1981; Rhum – Mussett 1984; Arran – Dickin, 1981; Ailsa Craig – Harrison et al 1987; Rockall – Hawkes et al, 1975; Mull - Chambers and Pringöle, 2001; Mourne - Gamble et al, 1999 Also shown are the Paleocene basic dykes.

Fig. 2. Gravity Anomaly Map of SW England (from BGS Gravity Anomaly Map 1, 1:500,000 (1997)). locations of the Lundy, Haig Fras and Cornubian gravity anomalies highlighted by white dashed lines. Reproduced with the permission of the British Geological Survey ©NERC. All rights Reserved

Fig. 3. Map of Lundy Island showing representative granite textures across the island and locations of all samples collected.

Fig. 4. Field photographs from Lundy Island. (a) Main Lundy granite cut by microgranite dykes and late pegmatites; The Cheeses; (b) xenolith of slate within the main Lundy granite; (c) trachyte dyke (green) cutting early doleritic dykes and in turn cut by a later basaltic dyke; Lundy south lighthouse; (d) faulted contact of the main Lundy granite with metasediments, Ladies beach; (e) faulted contact of main Lundy granite, cut by basalt dykes with metasediments at Rattles Anchorage.

Fig. 5. Geochemical tectonic discrimination diagrams (after Pearce et al., 1984), showing data from Thorpe et al. (1990) and Stone (1990). Red symbols represent analyses from Lundy; circles are granites, triangles are microgranites and pegmatites. Green symbols show analyses from Arran; triangles are microgranite, squares and circles respectively outer (coarse) and inner (fine) granite. Variscan Cornubian granites are shown in yellow with triangles, squares and circles respectively showing analyses from the Dartmoor megacrystic granite, Carnmenellis microgranite and Isles of Scilly microgranite.

Fig. 6. Element maps for garnets from the Lundy granite, showing Mn and Mg decreasing towards granet rim and Fe increasing towards the rim.

Fig. 7. Mica compositions from only coarse-grained megacrystic biotite granite compositions plotted in the nomenclature diagram of Tischendorf et al. (2001).

Fig. 8. Variations in tourmaline compositions. a) Backscattered electron image showing compositional variations in tourmaline. Analyses represent points along the lines A (rim) to C (core). b) Compositional variations from core (C) to rim (A). c-f) Cation occupancies in tourmaline (atoms per formula unit) in comparison to South West England (SWE, data from Müller et al., 2006).

Fig. 9. Selected cathodoluminescence images of zircon from Lundy granite and basic dyke samples.

Fig. 10. Inverse (Tera-Wasserburg) concordia diagrams for zircon from Lundy granite (a-e) and basic dyke (f, g) samples. Error ellipses are plotted at 2σ ; white filled ellipse in each panel is the concordia age (sensu Ludwig, 1998); dashed ellipses are analyses omitted from concordia age calculation.

Inherited grains and analyses rejected on the criterion of high common Pb are omitted for clarity. (h) Th-U systematics of the investigated zircon grains.

Fig. 11. Summary of geochronological data from Lundy samples.

References

- ANNEN, C., BLUNDY, J.D., & SPARKS, R.S.J. 2006. The Genesis of Intermediate and Silicic Magmas in Deep Crustal Hot Zones. *Journal of Petrology*. 47, 3, 505-539
- ARMSTRONG, J.T. 1995. CITZAF: A Package of Correction Programs for the Quantitative Electron Microbeam X-ray Analysis of Thick Polished Materials, Thin Films, and Particles Microbeam Analysis 4: 177-200.
- ARROWSMITH, S.J., KENDALL, M., WHITE, N, VANDECAR, J.C., BOOTH, D.C. 2006. Seismic Imaging of a hot upwelling beneath the British Isles. *Geology*. 33, 5, 345-348
- ARTHERTON, M. P. 1968. The variation in garnet, biotite and chlorite composition in medium grade pelitic rocks from the Dalradian, Scotland, with particular reference to the zonation in garnet. *Journal of Mineralogy and Petrology*, **18**, 347-371.
- ARTHUR, M. J. 1989. The Cenozoic evolution of the Lundy pull-apart basin into the Lundy rhomb horst. *Geological Magazine*. **126**, 187-98.
- BELL, J.D., 1976. The Tertiary intrusive complex on the Isle of Skye. *Proceedings of the Geological Association*. **87**, 247-71.
- BOTT, M. H. P, DAY, A.A., & MASSON SMITH, D, 1958. The geological interpretation of gravity and magnetic surveys in Devon and Cornwall. *Phil. Trans. R. Soc. Lond.* **A251**, 161-91
- BOTT, M. H.P. & TUSON, J., 1973. Deep structure beneath the Tertiary volcanic regions of Skye, Mull and Ardnamurchan, north-west Scotland, *Nature Phys. Sci.*, **242**, 114-1 16.
- BROOK, M. 1984. The age of the Conochair Granite. In: Harding et al. (1984) St. Kilda: an illustrated account of the geology. *Report of the British Geological Survey*, **(16)7**, 40-41.

- BROOKS, M. J., & THOMPSON, M. S., 1973. The geological interpretation of a gravity survey of the Bristol Channel. *J. Geol. Soc. Lond.* **129**, 245-74.
- BURNS, P.C., MACDONALD, D.J., and HAWTHORNE, F.C., 1994. The crystal chemistry of manganese-bearing elbaite. *Canadian Mineralogist*, 32, 31-41
- CHAMBERS, L. M. & FITTON, J. G. (2000). Geochemical transitions in the ancestral Iceland plume: evidence from the Isle of Mull Tertiary volcano, Scotland. *Journal of the Geological Society, London* 157, 261–263.
- CHAPPELL, B.W., & HINE, R., 2006, The Cornubian Batholith: An example of magmatic fractionation on a crustal scale. *Resource Geology*, **56**, 203–244, doi:10.1111/j.17513928.2006.tb00281.x.
- CHAPPELL, B.W., & WHITE, A.J.R., 1974, Two contrasting granite types: *Pacific Geology*, **8**, 173–174.
- CHAROY, B., 1986. The genesis of the Cornubian batholith (south-west England): the example of the Carnmenellis pluton. *J. Petrology* **27**, 571-604.
- CHELSEY, J.T., HALLIDAY, A.N., SNEE, L.W., MEZGER, K., SHEPHERD, T.J. & SCRIVENER, R.C. 1993. Thermochronology of the Cornubian batholith in SW England: implication for pluton emplacement and protracted hydrothermal mineralization. *Geochimica and Cosmochimica Acta*, **57**, 1817-1835.
- CHEN, Y., CLARK, A.H., FARRAR, E., WASTENEYS, H.A.H.P., HODGSON, M.J., & BROMLEY, A.V., 1993. Diachronous and independent histories of plutonism and mineralization in the Cornubian Batholith, southwest England. *Geological Society [London] Journal*, **150**, (6), 1183–1191, doi:10.1144/gsjgs.150.6.1183.
- CLEMENS, J.D. & STEVENS, G. 2012. What controls chemical variation in granitic magmas? *Lithos*, **134-135**, 317-329.
- CORNWELL, J. D., 1971. Geophysics of the Bristol Channel area, *Proc. Geol. Soc* **1664**, 286-289
- DANGERFIELD, J., 1982. The Tertiary igneous complex of Lundy. In *The Geology of Devon* (E. M. Durrance, M. and D. J. C. Laming, eds.). Univ. Exeter, pp. 238-48.
- DARBYBSHIRE, D. P. F., & SHEPHERD, T. J., 1985. Chronology of granite magmatism at associated mineralisation, S. W. England. *J. Geol. Soc. Lond.* 142, 1159-77

- DAVEY, F. J. 1970. Bouguer anomaly map of the North Celtic Sea and entrance to the Bristol Channel. *Geophys. J. R. Astr. Soc.* **2**, 277-82.
- DAVISON, E. H. 1932. The age of the Lundy Island granite. *Geol. Mag.* **69**, 76-7.
- DICKIN, A.P. 1981. Isotope geochemistry of Tertiary Igneous rocks from the isle of Skye, NW Scotland. *Journal of Petrology*, **22**, 155-189
- DODSON, M. H., & LONG, L. E., 1962. Age of Lundy granite, Bristol Channel. *Nature* **195**, 975-6.
- DOLLAR, A. T. J., 1941. The Lundy complex: its petrology and tectonics. *Q. J. Geol. Soc. London.* **97**, 39-77.
- DRIVENES, K., LARSEN, R.B., MÜLLER, A., SØRENSEN, B.E., WIEDENBECK, M., RAANES, M.P., 2015. Late-magmatic immiscibility during batholith formation: assessment of B isotopes and trace elements in tourmaline from the Land's End granite, SW England. *Contributions to Mineralogy and Petrology.* **169**, 56, doi:10.1007/s00410-015-1151-6.
- DUPUIS, N.E., BRAID, J.A., MURPHY, J.B., SHAIL, R.K., ARCHIBALD, D.A. & NANCE, R.D. 2015. ⁴⁰Ar/³⁹Ar phlogopite geochronology of lamprophyre dykes in Cornwall, UK: new age constraints on Early Permian post-collisional magmatism in the Rhenohercynian Zone, SW England. *Journal of the Geological Society*, **172**, 566-575.
- EDMONDS, E.A., WILLIAMS, B.J. & TAYLOR, R.T. 1979. Geology of Bideford and Lundy Island. Memoir of the Geological Survey of Great Britain, 129pp.
- EMELEUS, C. H. & BELL, B. R. 2005. British Regional Geology: the Palaeogene Volcanic Districts of Scotland, 4th ed.
- EXLEY, C.S. 1966. The Granitic Rocks of Haig Fras, Nature, **210**, 5034, pp. 365-367
- EXLEY, C.S., & STONE, M., 1982 Hercynian intrusive rocks. In: Sutherland, D. S. (ed.) *Igneous Rocks of the British Isles*. Chichester John Wiley, 287-320
- EXLEY, C.S., & FLOYD, P.A., 1983. Composition and petrogenesis of the Cornubian granite batholith and post-orogenic volcanic rocks in southwest England. In: Hancock, P.L. (ed.) *The Variscan Fold Belt in the British Isles*. Bristol: Adam Hilger, 153-77.
- FLOYD, P.A., EXLEY, C.S., & STYLES, M.T., 1993, *Igneous Rocks of South-West England: Geological Conservation Review Series*, Joint Nature Conservation Committee London, Chapman & Hall.

- GAMBLE, J.A., WYSOCZANKI, R.J. & MEIGHAN, I. G. 1999. Constraints on the age of the British Tertiary Volcanic Province from ion microprobe U-Pb (SHRIMP) ages for acid igneous rocks from NE Ireland. *Journal of the Geological Society*. **156**, 291-299
- GROMET, L. P. & SILVER, L. T. 1983. Rare earth distribution among minerals in a granodiorite and their petrogenetic implications. *Geochim. Cosmochim. Acta*, **47**, 925-39.
- HAMPTON, C. M, AND TAYLOR, P.N., 1983. The age and nature of the basement of southern Britain: evidence from Sr and Pb isotopes and granites. *J. Geol. Soc. Lond.* **140**, 499-509.
- HARRISON, R.K., STONE, P., CAMERON, I.B., ELLIOTT, R.W, HARDING, R.R. 1987. Geology, petrology and geochemistry of Ailsa Craig, Ayrshire. *Report on the British Geological Survey*, 16
- HAWKES, J.R. & DANGERFIELD, J. 1978. The Variscan granites of south-west England: a progress report. *Proc. Ussher Soc.*, **4**, 158-171.
- HAWKES, J.R., MERRIMAN, R.J., HARDING, R.R. & DARBYSHIRE, D.P.F. 1975. Rockall Island: new geological, petrological, chemical and Rb-Sr age data. In: Harrison R.K. (ed.) Expeditions to Rockall 1972-73. Institute of Geological Sciences Report No. 75/1, 15-51.
- HAWTHORNE, F.C. & HENRY, D.J. 1999. Classification of the minerals of the tourmaline group. *European Journal of Mineralogy*, **11**, 201-215
- HOLLISTER, L. S., 1966. Garnet zoning: an interpretation based on the Rayleigh fractionation model. *Science*, 154, 1647-1651
- HIPKIN, R. G., CHACKSFIELD, B. C, LYNESS, D., REAY, D., GIBBERD, A. J. & TURNBULL, G. 1986. Bouguer Anomaly Map of the British Isles, Southern Sheet, (1:625000). Keyworth: British Geological Survey.
- HUPPERT, H. E, & SPARKS, R. S. J., 1988. The fluid dynamics of crustal melting by injection of basaltic sills. *Trans. R. Soc. Edin. Earth Sci.* 79, 237-43.
- JEFFERIES, N. J. 1985. The distribution of the rare-earth elements in the Carnmenellis pluton. *Mineral. Mag.* **49**, 495-504.
- JONES, D.G., MILLER, J.M., ROBERTS, P.D. 1988. A seabed radiometric survey of Haig Fras, S.

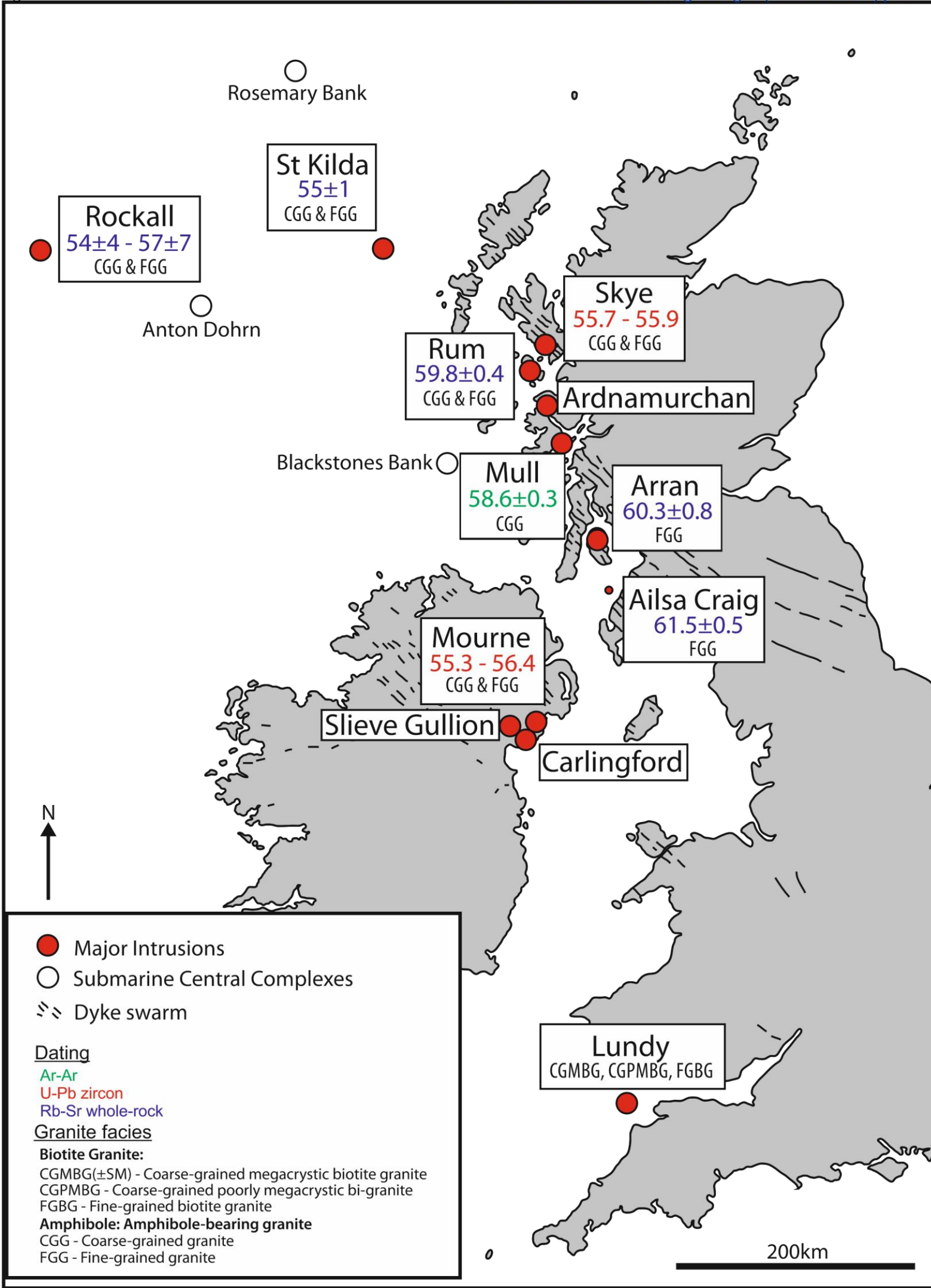
- Celtic Sea, U.K. *Proceedings of the Geologists Association*. **99(3)**, 193-203
- KENT, R.W. & FITTON, G. 2000, Mantle sources and melting dynamics in the British Palaeogene igneous province. *Journal of Petrology*, **41**, 1023-1040.
- LONDON, D., & MANNING, D.A.C., 1995. Chemical variation and significance of tourmaline from southwest England. *Economic Geology*, **90**, 495-519.
- LUDWIG, K.R. 1998. On the treatment of concordant uranium-lead ages. *Geochim. Cosmochim. Acta* **62**, 665-676.
- LUDWIG, K.R. 2012. User's Manual for Isoplot, 3.75. A geochronological toolkit for Microsoft Excel. Berkeley Geochronology Center Special Publication, No 5, 2455 Ridge Road, Berkeley CA, USA.
- MANSON, V., 1967. Geochemistry of Basaltic Rocks – Trace Elements: p215-269 in Hess, H.H. and Poldervaart, A. (Eds.) – Basalts: Interscience Publishers, New York, 862p.
- MCCAFFREY, R., STEWART, P., DALZELL, P., MCCAFFREY, L. & MCELROY, J. 1993. A reconnaissance magnetic survey of the Lundy Tertiary Igneous Complex, Bristol Channel. *Proceedings of the Ussher Society*, **8**, 193-197.
- MCLAREN, A.C., FITZGERALD, J.D., & WILLIAMS, I.S., 1994. The microstructure of zircon and its influence on the age determination from Pb/U isotopic ratios measured by ion micro-probe. *Geochim. Cosmochim. Acta* **58**, 993–100.
- MEIGHAN, L G., 1979. The acid igneous rocks of the British Tertiary Province. *Bull. Geol. Surv. Great Britain*. **70**, 10-22.
- MEIGHAN, L.G, GIBSON, D, & HOOD, D. N., 1984. Some aspects of Tertiary magmatism in NE Ireland. *Miner. Mag.* **48**, 351-63.
- MILLER, J.A, & FITCH, F.J., 1962. Age of the Lundy granites. *Nature*. **195**, 553-5.
- MITTFELDEHLDT, D.W. & MILLER, C.A. 1983. Geochemistry of the Sweetwater Wash pluton, California: implications for 'anomalous' trace element behaviour during differentiation of felsic magmas. *Geochim. Cosmochim. Acta*, **47**, 109-24.

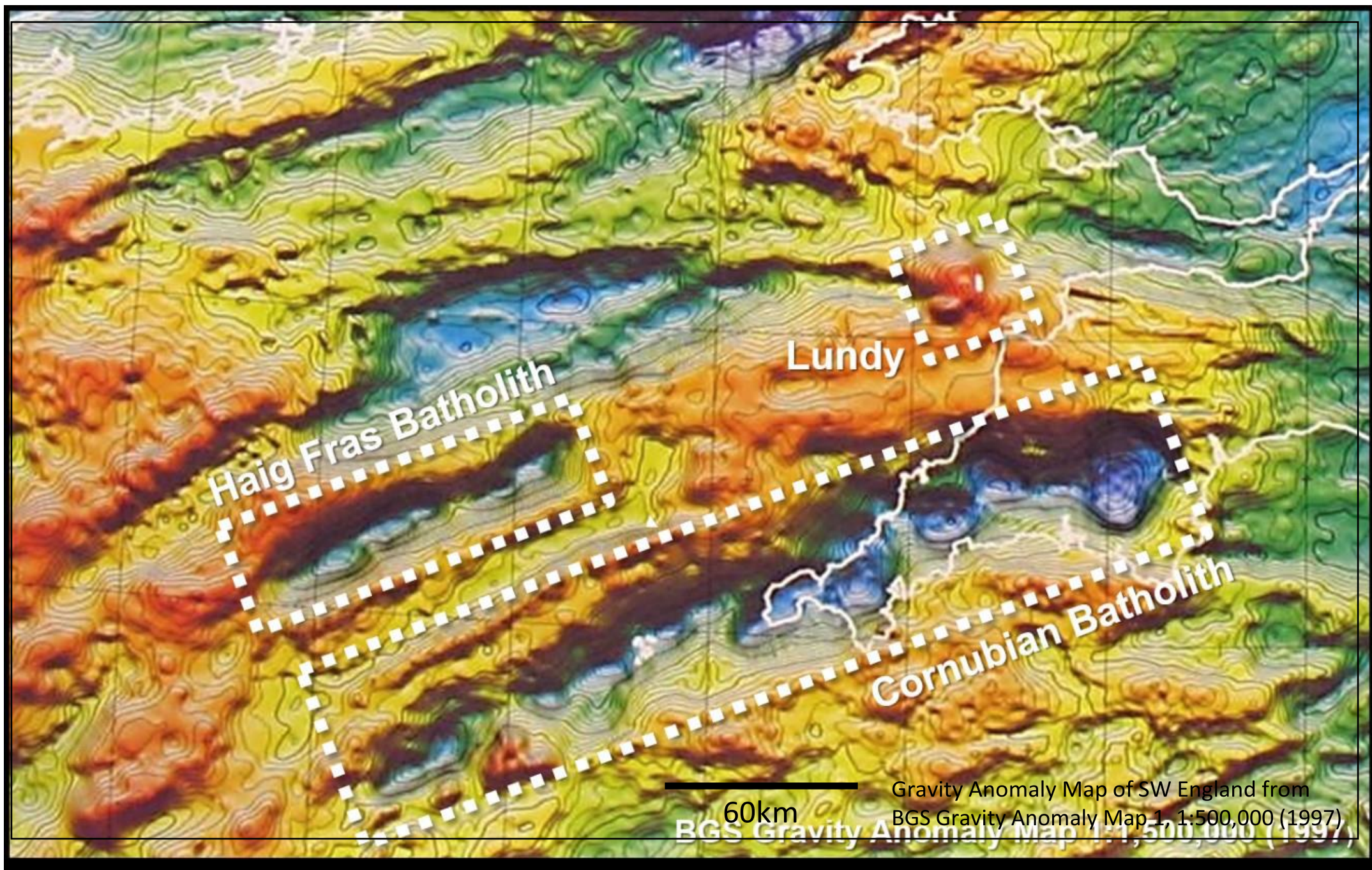
- MOORBATH, S. & BELL, J.D. 1965. Strontium isotope abundance studies and rubidium-strontium age determinations on Tertiary igneous rocks from the Isle of Skye, northwest Scotland. *Journal of Petrology*, **6**(1), 37-66.
- MÜLLER, A., SELTMANN, R., HALLS, C., SIEBEL, W., DULSKI, P., JEFFRIES, T., SPRATT, J., KRONZ, A. 2006. The magmatic evolution of the Land's End Pluton, Cornwall, and associated pre-enrichment of metals. *Ore geology reviews*, **28**, 329-367.
- MUSSETT, A. E. 1984. Time and duration of Tertiary igneous activity of Rhum and adjacent areas. *Scottish Journal of Geology*, **20**, 273-279.
- MUSSETT, A.E., DAGLEY, P. & ECKFORD, M. 1976. The British Tertiary Igneous Province: palaeomagnetism and ages of dykes, Lundy Island, Bristol Channel. *Geophysical Journal of the Royal Astronomical Society*, **46**, 595-603.
- MUSSETT, A. E, DAGLEY, P, & SKELHORN, R. R. 1988. Time and duration of activity in the British Tertiary Igneous Province. 337–348 in Early Tertiary volcanism and the opening of the North Atlantic. Morton, A.C., & Parson, L.M. (editors). *Geological Society of London Special Publication*, **39**.
- NANCE, R.D., NEACE, E.R., BRAID, J.A., MURPHY, J.B., DUPUIS, N. & SHAIL, R.K. 2015. Does the Meguma Terrane Extend into SW England? *Geoscience Canada*, **42**, 61-76, doi:10.12789/geocanj.2014.41.056.
- NEACE, E.R. NANCE, R.D, MURPHY, J.B., LANCASTER, P.J., & SHAIL, R.K. 2016. Zircon LAICPMS geochronology of the Cornubian Batholith, SW England. *Tectonophysics* **681**, 332–352.
- PEARCE, J.A., HARRIS, N.B.W, & TINDLE, A.G., 1984. Trace element discrimination diagrams for the tectonic interpretation-of granitic rocks. *J. Petrology*, **25**, 956-83
- POWNALL, J.M., WATERS, D.J., SEARLE, M.P., SHAIL, R.K., & ROBB, L.J., 2012. Shallow laccolithic emplacement of the Land's End and Tregonning granites, Cornwall, UK: evidence from aureole field relations and P–T modeling of cordierite-anthophyllite hornfels. *Geosphere*, **8**,1467–1504. doi:10.1130/ges00802.1
- PRINZ, M., 1967. Geochemistry of Basaltic Rocks – Trace Elements: p271-323 in Hess, H.H. and Poldervaart, A. (Eds.) – Basalts: Interscience Publishers, New York, 862p.

- ROBERTS, C. L. & SMITH, S.G. 1994. A new magnetic survey of Lundy Island, Bristol Channel. *Proceedings of the Ussher Society*, **8**, 293-297.
- ROMER., R.L. & KRONER, U. 2016. Phanerozoic tin and tungsten mineralization—tectonic controls on the distribution of enriched protoliths and heat sources for crustal melting. *Gondwana Research*, 31, pp. 60–9
- SHAIL, R.K., & LEVERIDGE, B.E., 2009, The Rhenohercynian passive margin of SW England: Development, inversion and extensional reactivation: *Comptes Rendus Geoscience*, **341** (2–3), 140–155, doi:10.1016/j.crte.2008.11.002.
- SHELLEY, D., 1966. The significance of granophyric and myrmekitic textures in the Lundy granites. *Miner. Mag.* **35**, 678-91.
- SIMONS, B.J., SHAIL R.K., ANDERSEN J., 2016. The petrogenesis of the Early Permian Variscan granites of the Cornubian Batholith: Lower plate post-collisional peraluminous magmatism in the Rhenohercynian Zone of SW England, *Lithos*, volume 260, pages 76-94,
- SPEIGHT, J.M., SKELHORN, R.R., SLOAN, T. & KNAAP, R.J. 1982. The dyke swarms of Scotland. In: Igneous rocks of the British Isles. Ed: D.S. Sutherland, John Wiley and Sons, Chichester, 449-45
- STACEY, J.S. & KRAMERS, J.D. 1975. Approximation of Terrestrial Lead Isotope Evolution by a 2-Stage Model. *Earth and Planetary Science Letters*, **26**(2): 207-221.
- STEIGER, R. H. & JAGER, E. 1977. Subcommittee on geochronology: convention on the use of decay constants in geo- and cosmochronology. *Earth and Planetary Science Letters*, 36, 359–362.
- STONE, M. 1987. Geochemistry and origin of the Carnmenellis pluton, Cornwall: further considerations. *Proc. Ussher Soc.* **6**, 454-60.
- STONE, M., 1988. The significance of almandine garnets in the Lundy and Dartmoor granites. *Mineral. Mag.* **52**, 651-8.
- STONE, M. 1990. The Lundy granite: a geochemical and petrogenetic comparison with Hercynian and Tertiary granites. *Mineralogical Magazine* **54**, 431-446
- STONE, M., & EXLEY, C.S. 1989. Geochemistry of the Isles of Scilly pluton. *Proc. Ussher Soc.* **7**, 152-7.

- TAPPIN, D.R., CHADWICK, R.A., JACKSON, A.A., WINGFIELD, R.T.R. & SMITH, N.J.P. 1994. *United Kingdom offshore regional report: the geology of Cardigan Bay and the Bristol Channel. HMSO for the British Geological Survey, London.*
- TEGNER, C., BROOKS, C.K., DUNCAN, R.A., HEISTER, L.E., BERNSTEIN, S. 2008. 40Ar-39Ar ages of intrusions in East Greenland: rift-to-drift transition over the Iceland hotspot. *Lithos* **101**, 480-500.
- THOMPSON, R.N. 1982. Magmatism of the British Tertiary Volcanic Province. *Scot. J. Geol.* **18**, 491-7.
- THOMPSON, R.N. & MORRISON, M.A. 1988. Asthenospheric and lower-lithospheric mantle contributions to continental extensional magmatism: An example from the British Tertiary Province. *Chemical Geology*. **68**, pp 1-5.
- THORPE, R.S. 1978. The parental basaltic magma of granites from the Isle of Skye, NW Scotland. *Mineral. Mag.* **42**, 157-8.
- THORPE, R.S. & TINDLE, A.G. 1992. The petrology and petrogenesis of a Tertiary bimodal dolerite-peralkaline/subalkaline trachyte/rhyolite dyke association from Lundy (Bristol Channel, U.K.). *Geol. Jour.*, **27**, 101-117.
- THORPE, R. S., TINDLE, A. G. & GLEDHILL, A. 1990. The petrology and origin of the Tertiary Lundy granite (Bristol Channel, U.K.). *Journal of Petrology* **31**, 1379- 1406.
- TISCHENDORF, G., FÖRSTER, H-J., & GOTTESMANN, B., 2001. Minor- and trace-element composition of trioctahedral micas: a review. *Mineralogical Magazine* **65**, 249 – 276.
- WALSH, J.N. & CLARKE, E. 1982. The role of fractional crystallization in the formation of granitic and intermediate rocks of the Beinn Chaisgidle centre, Mull, Scotland. *Mineral. Mag.* **45**, 247-55.
- WAGER, L. & BROWN, 1968. Layered Igneous Rocks. Oliver & Boyd, London. 588 pp.
- WHITE, A. J. R., & CHAPPELL, B. N, 1988. Some supracrustal (S-type) granites of the Lachlan fold belt Trans. R. Soc. Edin. Earth Sci. **79**, 169-81
- WHITE, R., & MCKENZIE, D. 1989. Magmatism at rift zones: The generation of volcanic continental margins and flood basalts. *J. Geophys. Res.* **94(B6)**, 7685–7729.

- WHITEHOUSE, M.J., KAMBER, B. & MOORBATH, S., 1999. Age significance of U–Th–Pb zircon data from early Archaean rocks of west Greenland: a reassessment based on combined ion-microprobe and imaging studies. *Chemical Geology*, **160**, 201–224.
- WHITEHOUSE, M.J. & KAMBER, B.S. 2005 Assigning dates to thin Gneissic veins in high-grade metamorphic terranes: A cautionary tale from Akilia, southwest Greenland, *J. Petrol.*, **46**(2), 291–318. doi: 10.1093/petrology/egh075
- WIEDENBECK, M., ALLE, P., CORFU, F., GRIFFIN, W. L., MEIER, M., OBERLI, F., VON QUADT, A., RODDICK, J.C. & SPIEGEL, W. 1995. Three natural zircon standards for U–Th–Pb Lu–Hf trace element and REE analysis. *Geostandards Newsletter*, **19**, 1–23.
- WOODCOCK, N.H., SOPER, N.J., STRACHAN, R.A., 2007. A Rheic cause for the Acadian deformation in Europe. *Journal of the Geological Society of London* **164**, 1023–1036.
- ZECK, H. P. & WHITEHOUSE, M. J. 1999. Hercynian, Pan-African, Proterozoic and Archean ionmicroprobe zircon ages for a Betic-Rif core complex, Alpine belt, W. Mediterranean – consequences for its P–T–t path. *Contributions to Mineralogy and Petrology*, **134**, 134–49.
- ZEN, E. 1986. Aluminium enrichment in silicic melts by fractional crystallization: some mineralogic and petrographic constraints. *J. Petrol.* **21**, 1095–117





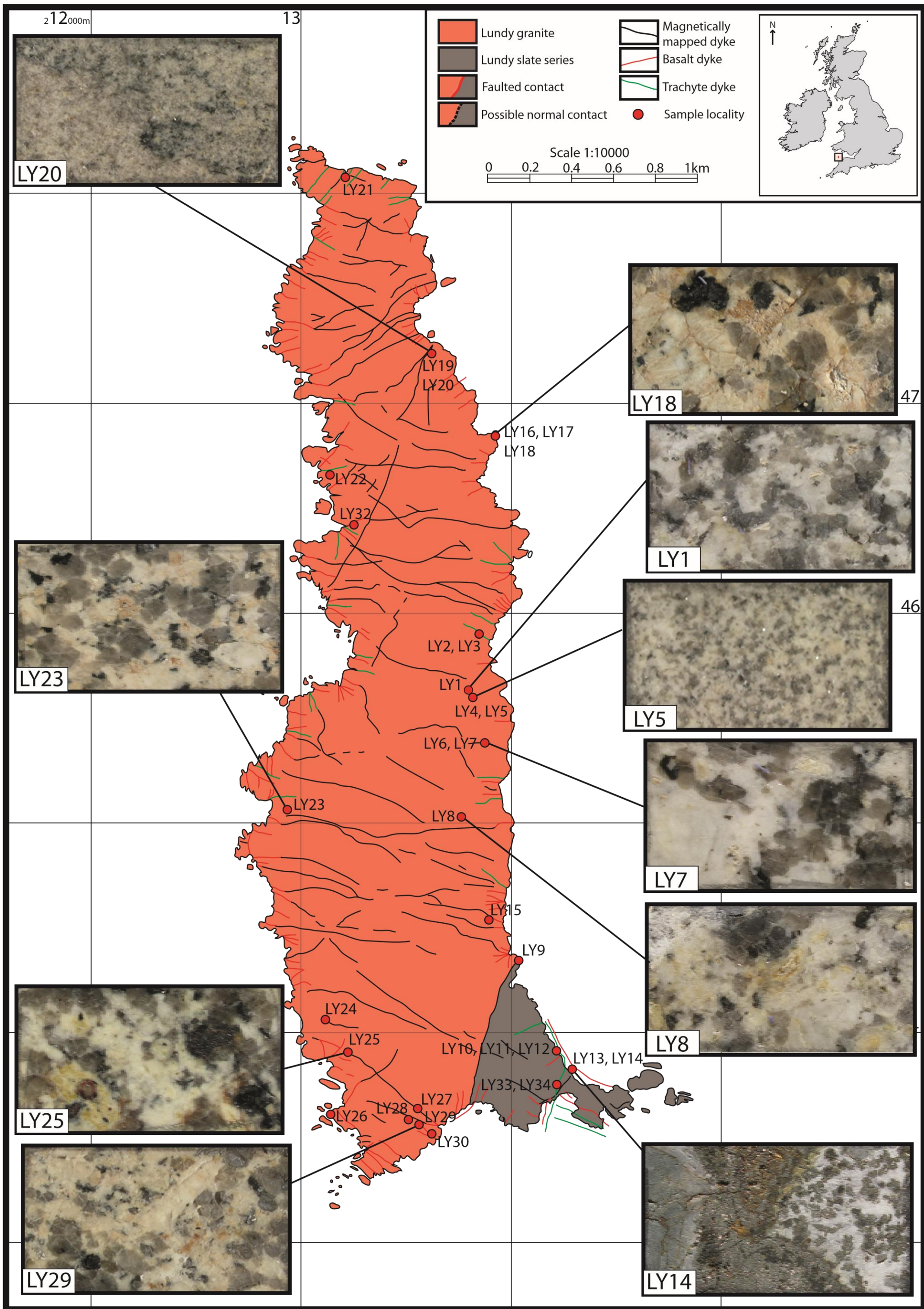


Fig. 4. Field photos

[Click here to download Figure Fig. 4 \(Field Photos Summary\).pdf](#)

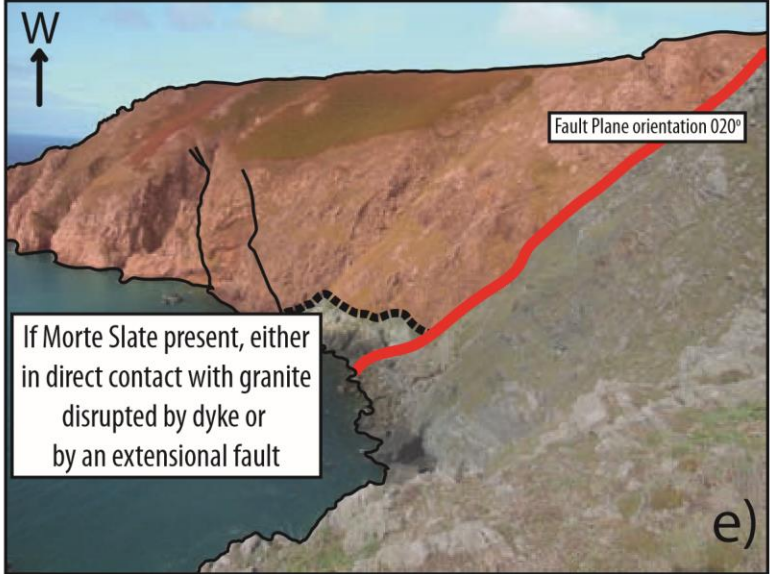
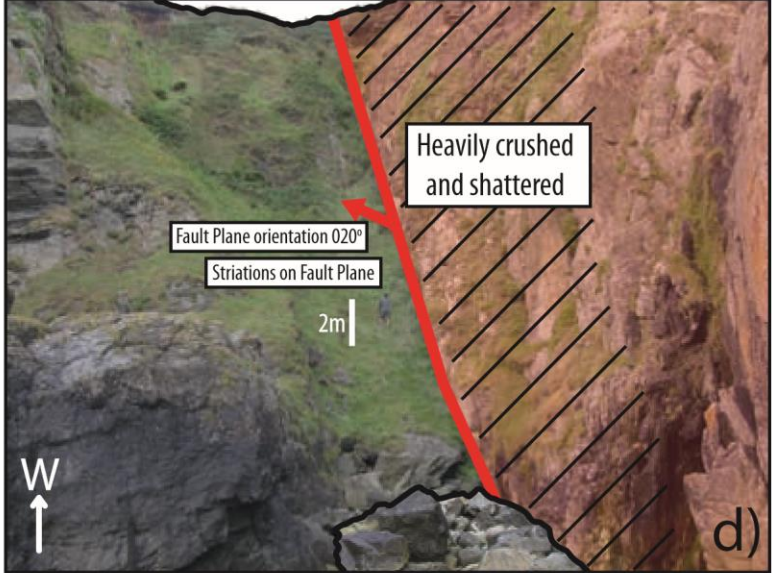
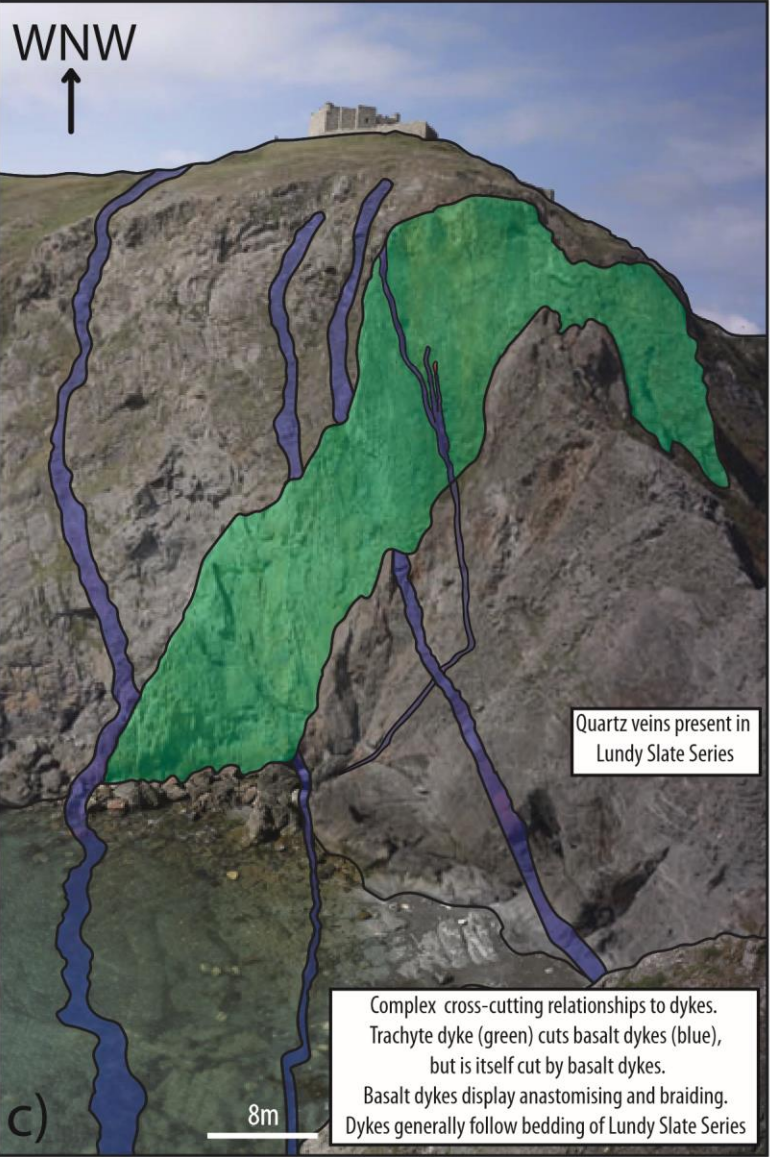
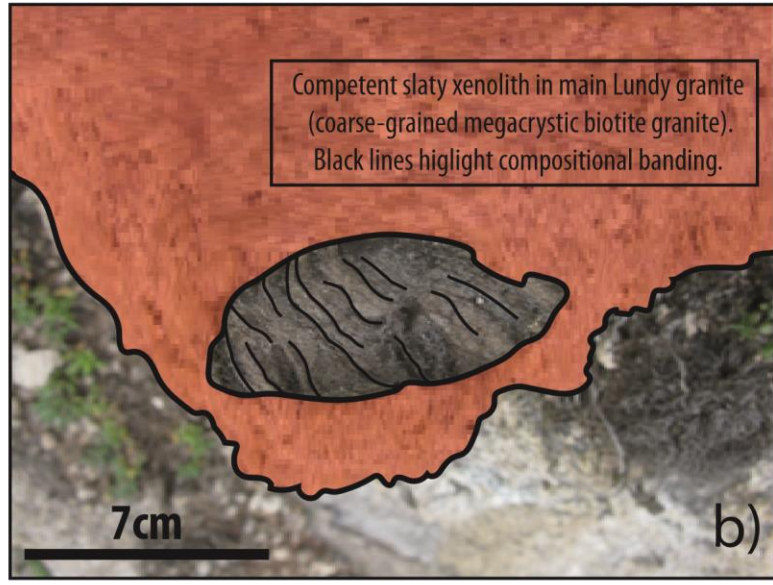
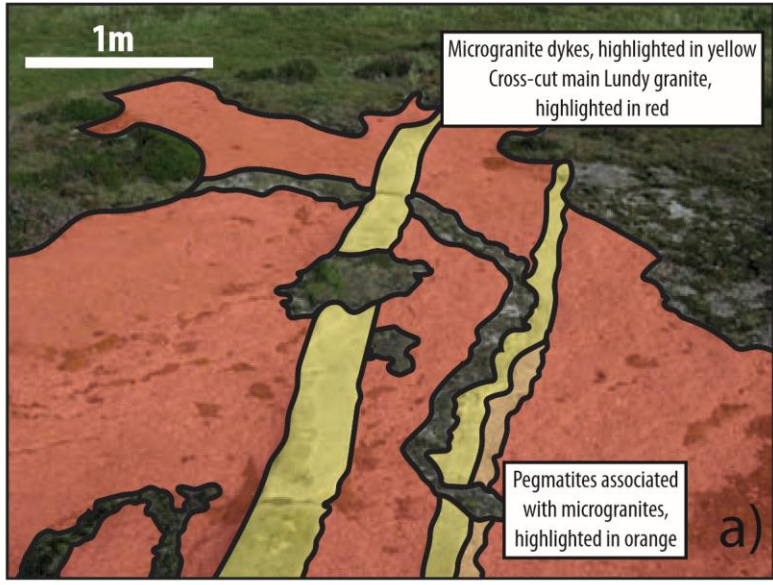
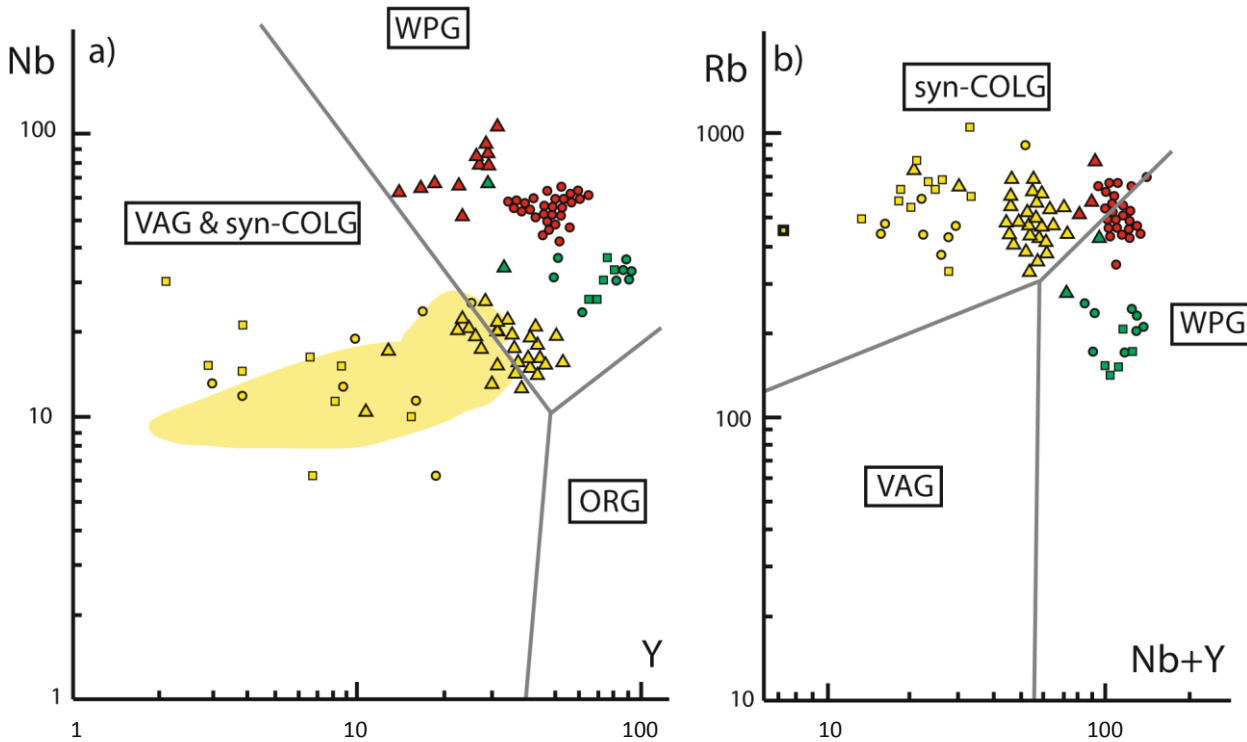


Fig. 5. Geochem. discrimination plots

[Click here to download Figure Fig. 5 \(tectonic discr diagrams\).pdf](#)



- ▲ ● Lundy granite
- ▲ ■ ● Arran microgranite, outer (coarse) and inner (fine) granite respectively
- ▲ Dartmoor Biotite megacrystic granite
- Carnmenellis microgranite
- Isles of Scilly microgranite

Fig. 6. Garnet maps

[Click here to download Figure Fig. 6 \(Garnet Maps\)-v2.pdf](#)

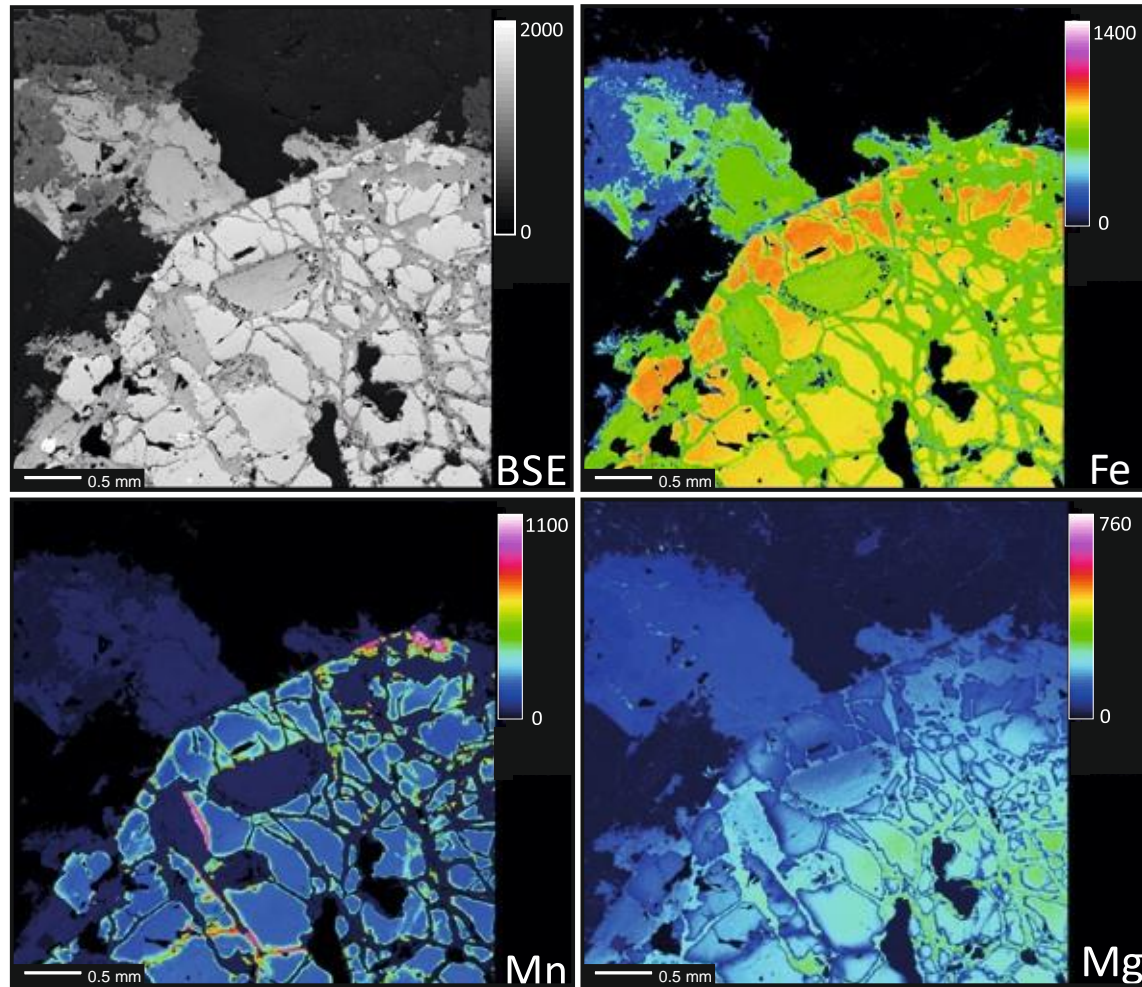


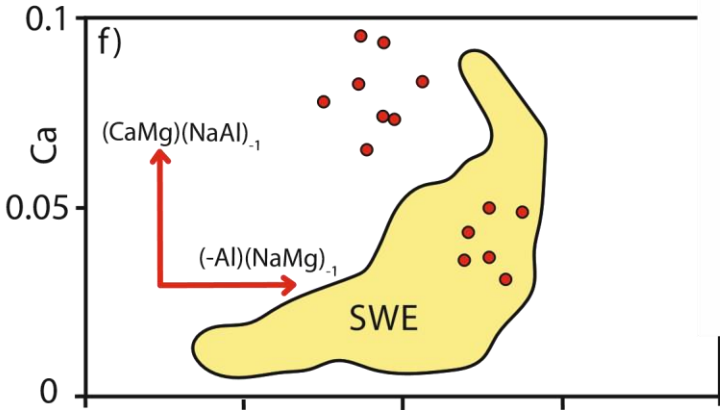
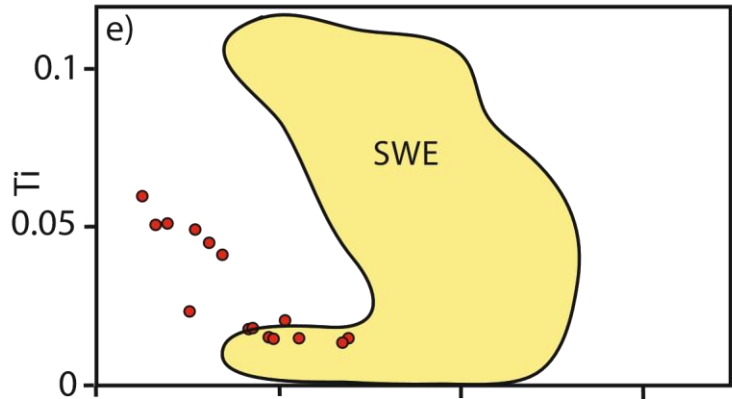
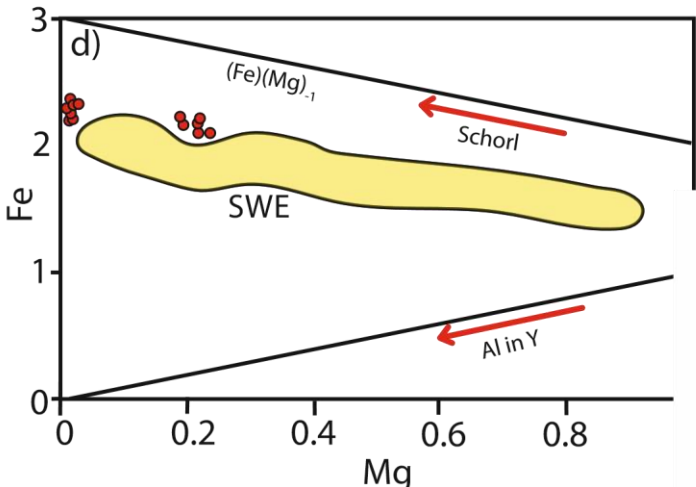
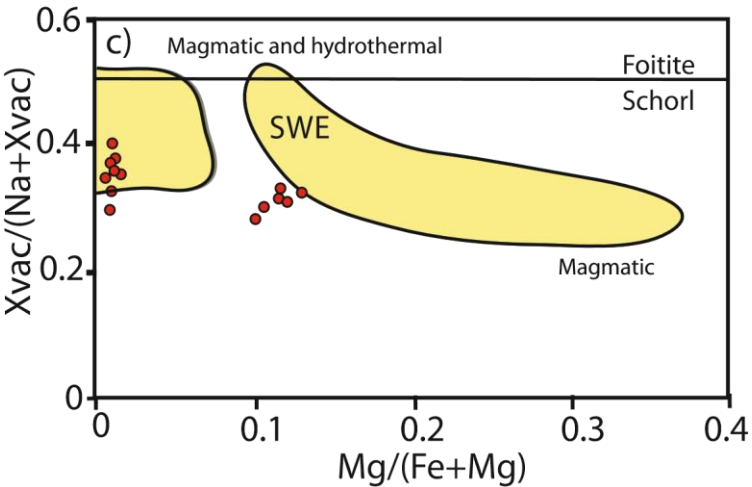
Fig. 7. Mica compositions

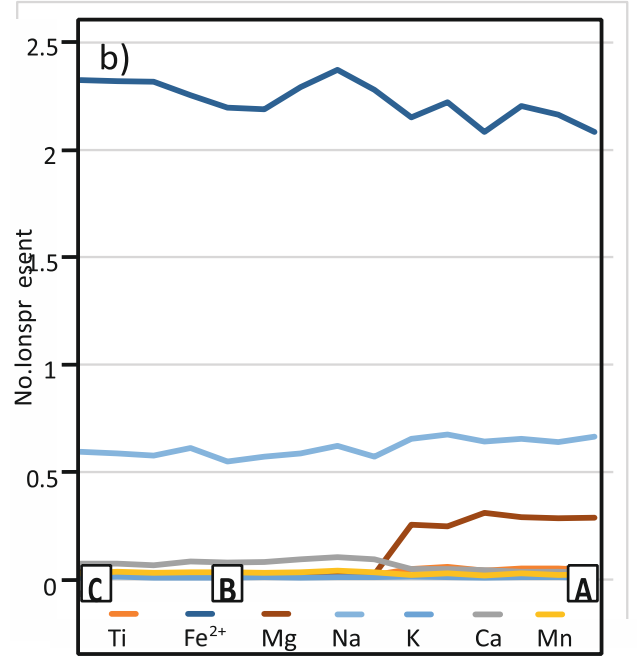
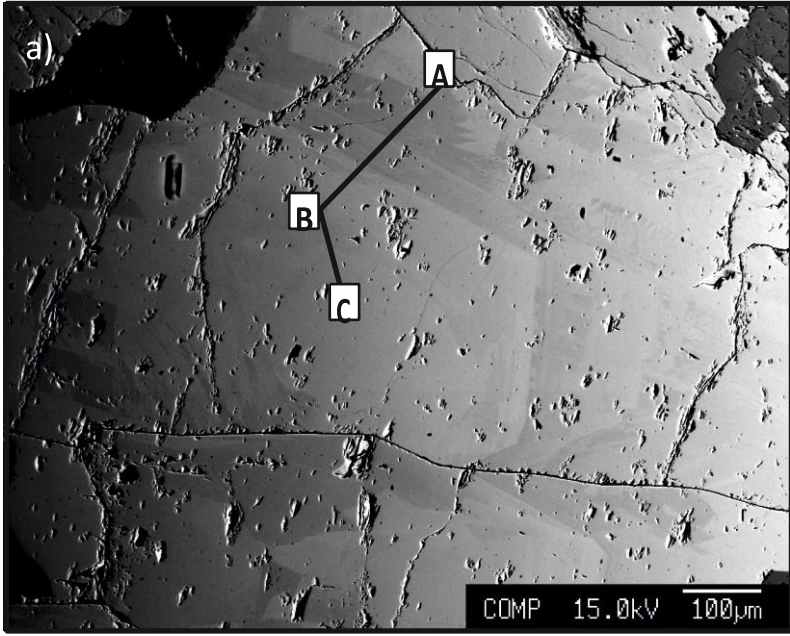
[Click here to download Figure Fig. 7 \(Micas\).pdf](#)



Fig. 8. Tourmaline compositions

[Click here to download Figure Fig. 8 \(tourmaline\).pdf](#)





0.3 0.5 0.7 0.9

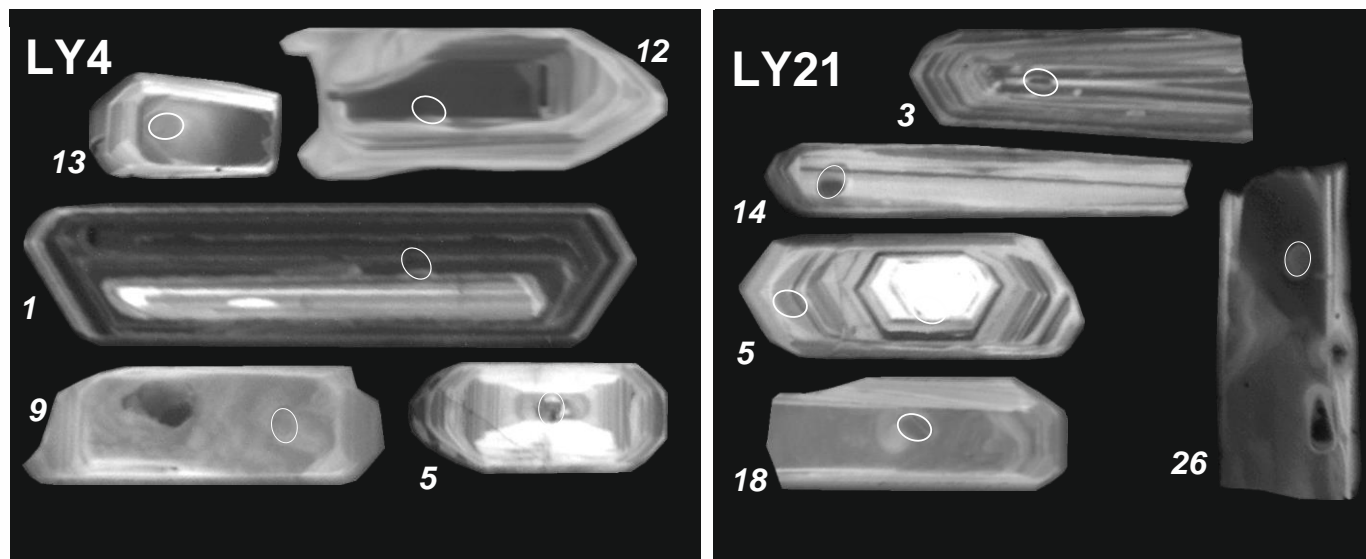
Al in Y

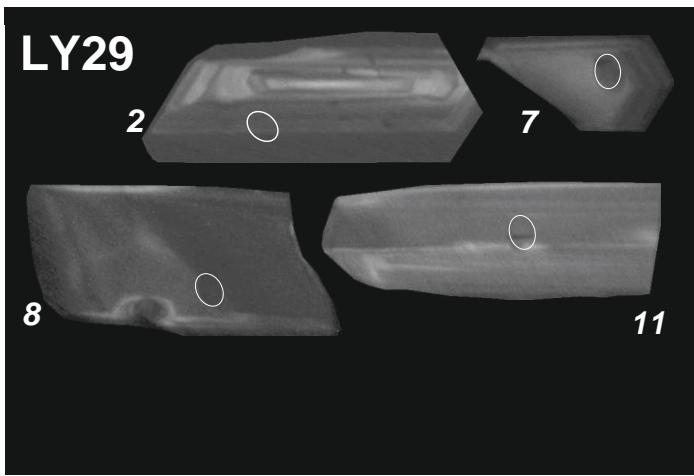
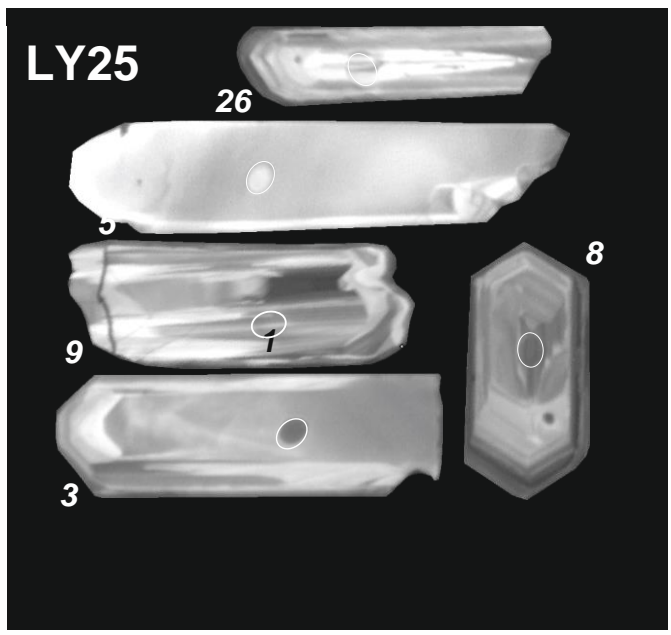
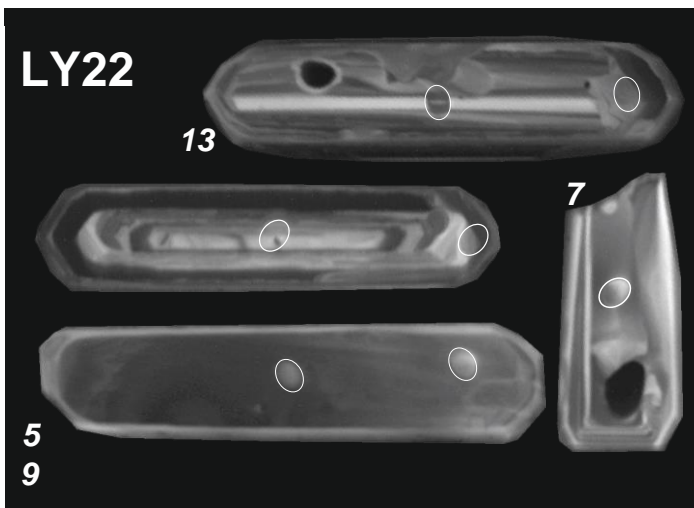
0.4 0.5 0.6 0.7 0.8

Na

Fig. 9. CL images

[Click here to download Figure Fig. 9 \(CL images\).pdf](#)





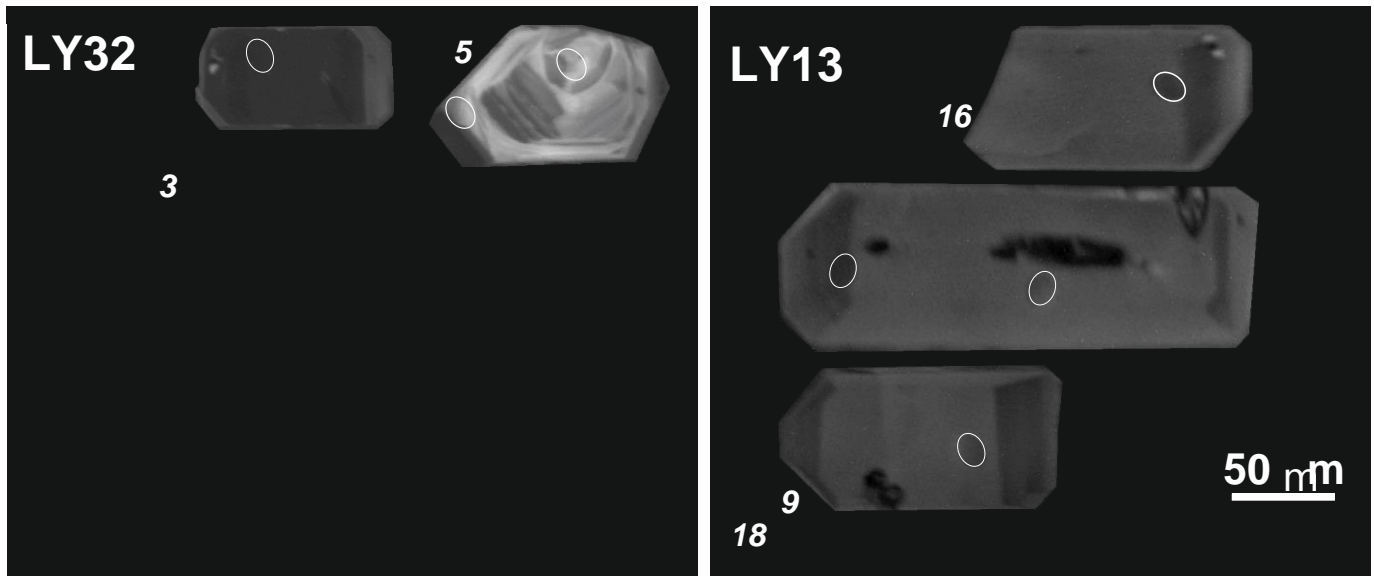
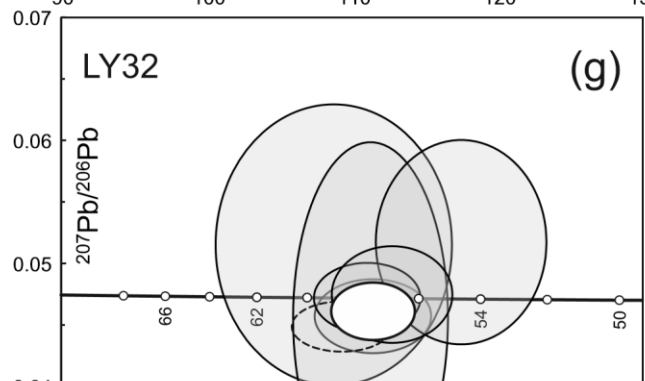
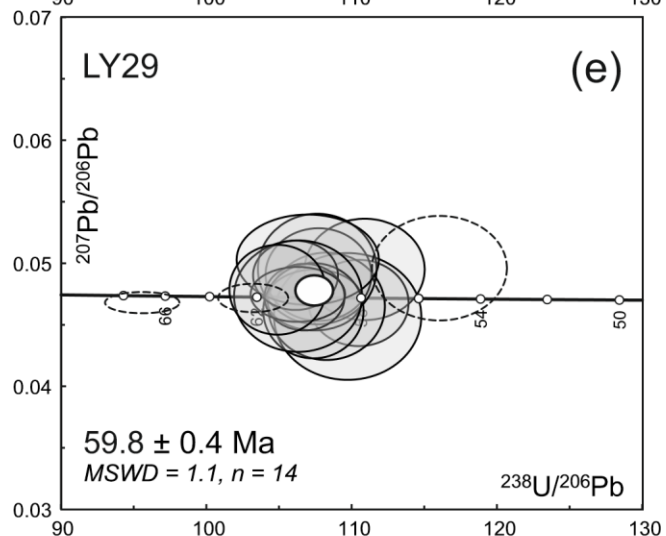
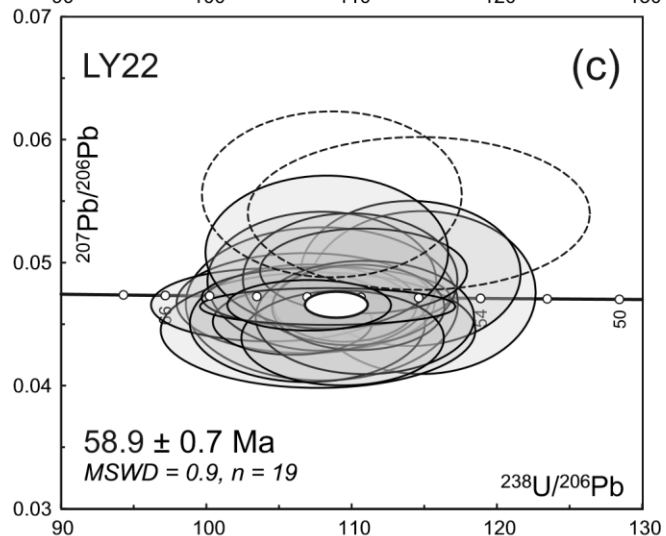
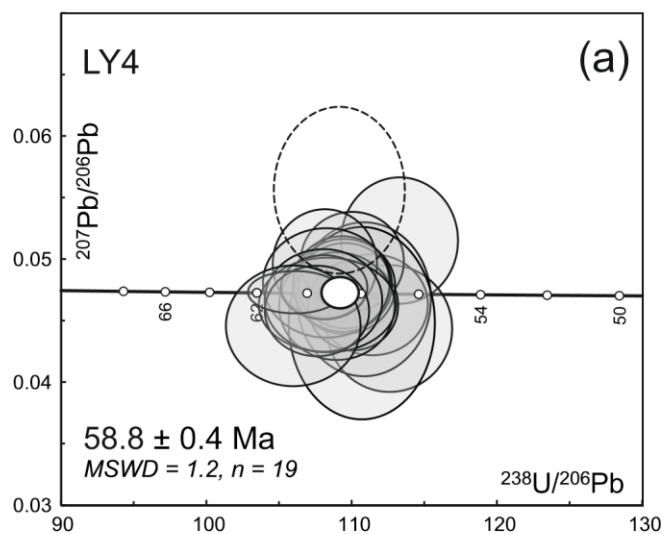
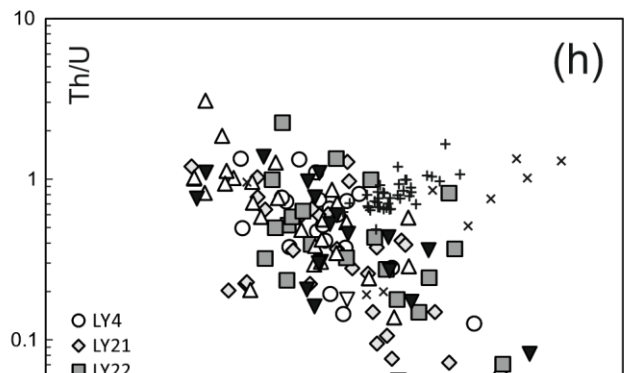
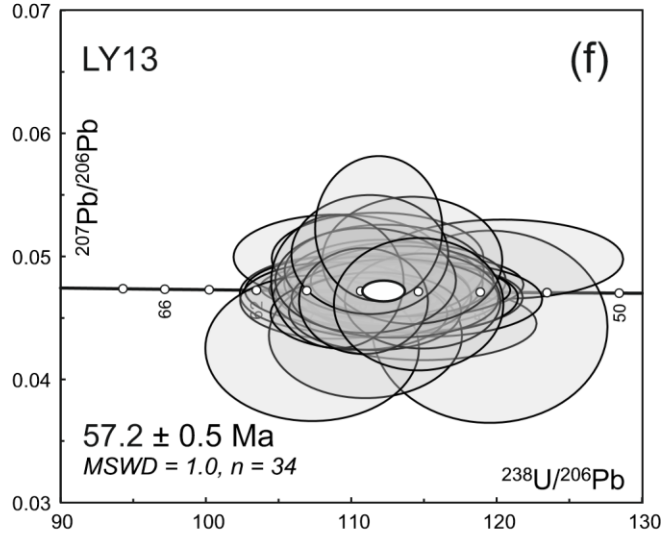
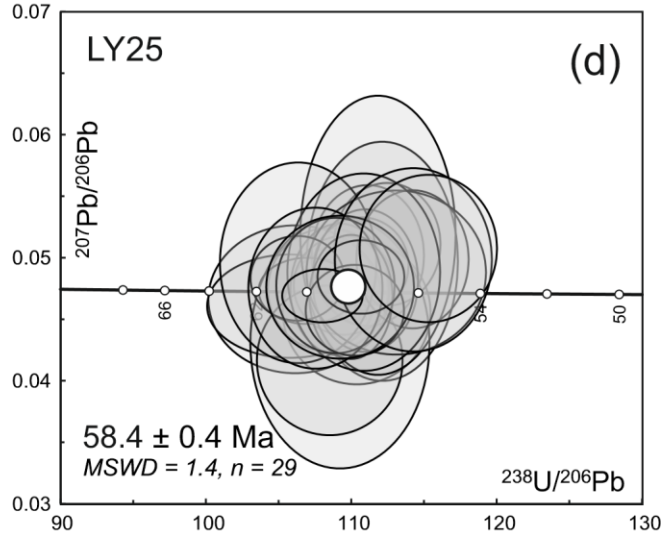
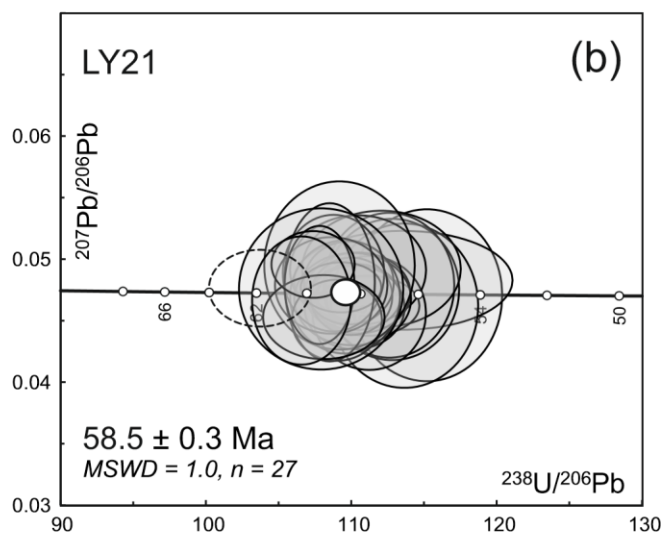


Fig. 10. Concordia plots





90
10000

100

110

120

130

10

100

1000

Fig. 11. Geochron. summary

[Click here to download Figure Fig. 11 \(age summary\).pdf](#)

